Cyclin A-cdk1-Dependent Phosphorylation of Bora Is the Triggering Factor Promoting Mitotic Entry

Suzanne Vigneron, Lena Sundermann, Jean-Claude Labbé, Lionel Pintard, Ovidiu Radulescu, Anna Castro, Thierry Lorca

Article

Developmental Cell

Cyclin A-cdk1-Dependent Phosphorylation of Bora Is the Triggering Factor Promoting Mitotic Entry

Graphical Abstract

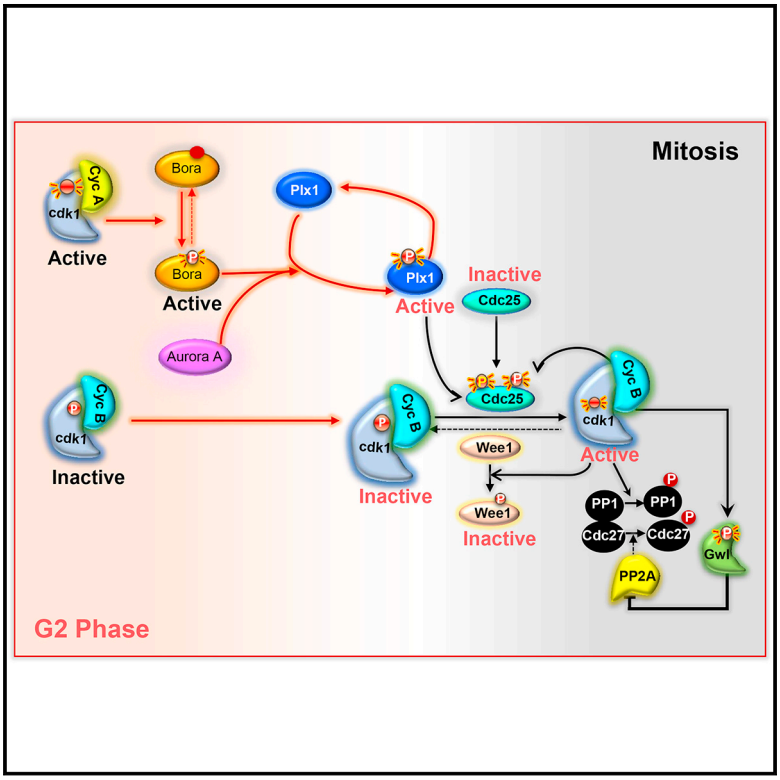

Highlights

- Unlike cyclin B/cdk, cyclin A/cdk1 is not inhibited by Wee1 during interphase
- The active cyclin A/cdk1 complex phosphorylates Bora and promotes Plx1 activation
- Plx1 initiates a cyclin B/cdk1 positive feedback loop promoting mitotic entry
- Cyclin A/cdk1 is the triggering factor promoting mitotic commitment

Authors

Suzanne Vigneron, Lena Sundermann, Jean-Claude Labbé, Lionel Pintard, Ovidiu Radulescu, Anna Castro, Thierry Lorca

Correspondence

anna.castro@crbm.cnrs.fr (A.C.), thierry.lorca@crbm.cnrs.fr (T.L.)

In Brief

Mitotic commitment was thought to depend on the accumulation of cyclin B/cdk1 during G2. Vigneron et al. now revise this view by showing that the key event triggering mitotic entry depends instead on cyclin A/cdk1, which phosphorylates Bora, leading to activation of Plk1 and a cyclin B/cdk positive feedback loop.

Vigneron et al., 2018, Developmental Cell *45*, 637–650
June 4, 2018
https://doi.org/10.1016/j.devcel.2018.05.005

CellPress

Developmental Cell
Article

Cyclin A-cdk1-Dependent Phosphorylation of Bora Is the Triggering Factor Promoting Mitotic Entry

Suzanne Vigneron,[1] Lena Sundermann,[1] Jean-Claude Labbé,[1] Lionel Pintard,[2] Ovidiu Radulescu,[3] Anna Castro,[1,*] and Thierry Lorca[1,4,*]

[1]Centre de Recherche de Biologie cellulaire de Montpellier (CRBM), CNRS UMR 5237, Université de Montpellier, 1919 Route de Mende, 34293 Montpellier Cedex 5, France

[2]Equipe Labelisée Ligue Contre le Cancer, Institut Jacques Monod, UMR7592, Université Paris-Diderot, Sorbonne Paris Cité, CNRS, Paris, France

[3]Dynamique des Interactions Membranaires Normales et Pathologiques (DIMNP), CNRS UMR5235, Université de Montpellier, Place E Bataillon, 34095 Montpellier, France

[4]Lead Contact

*Correspondence: anna.castro@crbm.cnrs.fr (A.C.), thierry.lorca@crbm.cnrs.fr (T.L.)

https://doi.org/10.1016/j.devcel.2018.05.005

SUMMARY

Mitosis is induced by the activation of the cyclin B/cdk1 feedback loop that creates a bistable state. The triggering factor promoting active cyclin B/cdk1 switch has been assigned to cyclin B/cdk1 accumulation during G2. However, this complex is rapidly inactivated by Wee1/Myt1-dependent phosphorylation of cdk1 making unlikely a triggering role of this kinase in mitotic commitment. Here we show that cyclin A/cdk1 kinase is the factor triggering mitosis. Cyclin A/cdk1 phosphorylates Bora to promote Aurora A-dependent Plk1 phosphorylation and activation and mitotic entry. We demonstrate that Bora phosphorylation by cyclin A/cdk1 is both necessary and sufficient for mitotic commitment. Finally, we identify a site in Bora whose phosphorylation by cyclin A/cdk1 is required for mitotic entry. We constructed a mathematical model confirming the essential role of this kinase in mitotic commitment. Overall, our results uncover the molecular mechanism by which cyclin A/cdk1 triggers mitotic entry.

INTRODUCTION

Cell division involves the coordination of different key events that ensure correct genetic duplication and transmission. As such, mitosis commitment must only take place once DNA replication is completed. Entry into mitosis is triggered by the rapid activation of cyclin B/cdk1 and Greatwall (Gwl) kinases, which respectively promote massive protein phosphorylation and counteract protein dephosphorylation via the inhibition of the phosphatase PP2A-B55 (Burgess et al., 2010; Gharbi-Ayachi et al., 2010; Vigneron et al., 2009). During G2, cyclin B-cdk1 is maintained inactive by Wee1/Myt1-dependent inhibitory phosphorylations on threonine 14 (T14) and tyrosine 15 (Tyr15) of cdk1 while PP2A-B55 is maintained active. Entry into mitosis is induced by the Cdc25 phosphatase that promotes the dephosphorylation of these two residues and cyclin B-cdk1 activation. Current models propose that, at mitotic entry, a partial amount of active cyclin B-cdk1 triggers a feedback loop by phosphorylating Wee1/Myt1 and Cdc25, thereby activating Cdc25 and inactivating Wee1/Myt1 (Pomerening et al., 2005; Sha et al., 2003). This feedback loop also includes a cdk-dependent activation of Gwl that leads to PP2A-B55 inhibition (Mochida et al., 2016). The trigger of the cyclin B/cdk1 and PP2A-B55 double-activation loop results in a bistable switch activation that promotes rapid and irreversible mitotic entry (Mochida et al., 2016).

Despite considerable progress, the factor triggering cyclin B/cdk1 activation is still elusive. This factor has been attributed to the accumulation of cyclin B (Deibler and Kirschner, 2010; Tuck et al., 2013), but how cyclin B accumulation could lead to cyclin B/cdk1 activation that would escape inhibitory regulatory phosphorylations is completely unknown.

The evolutionarily conserved Polo-like kinase (Plk1) is a good candidate for triggering mitotic entry. Plk1 is activated by phosphorylation of its activation loop on threonine 210 in humans/threonine 201 in *Xenopus* (T201) (Jang et al., 2002) during G2 preceding cyclin B/cdk1 activity (Gheghiani et al., 2017) and its disruption has been shown to block cells in G2 (Gheghiani et al., 2017; Lane and Nigg, 1996). Plk1 phosphorylates Cdc25B (Lobjois et al., 2011), Cdc25C (Roshak et al., 2000), Wee1 (Watanabe et al., 2005), and Myt1 (Nakajima et al., 2003) *in vitro* and it has been shown to trigger Cdc25C phosphorylation and activation *in cellulo* (Gheghiani et al., 2017). Previous studies reported a role of the Plkk1 kinase in Plk1 activation during G2 (Qian et al., 1998), while recent data support that Plk1 phosphorylation on T210 is mediated in human cells by the kinase Aurora A and requires the cofactor Bora (Macurek et al., 2008; Seki et al., 2008). Interestingly, Bora phosphorylation by cdk greatly enhances Plk1 phosphorylation by Aurora A (Chan et al., 2008; Tavernier et al., 2015; Thomas et al., 2016), supporting a role of an upstream cdk activity for Plk1 and cyclin B/cdk1 activation. This key cdk activity could be cyclin A-cdk. Accordingly, cyclin A/cdk complex displays two peaks of activity, one in S phase and a second one progressively increasing during G2 (Goldstone et al., 2001; Pagano et al., 1992). It is well accepted that cyclin A/cdk plays a major role in S phase by controlling Cdc45 and Cdc6 activities (Woo and Poon, 2003). Likewise, although several

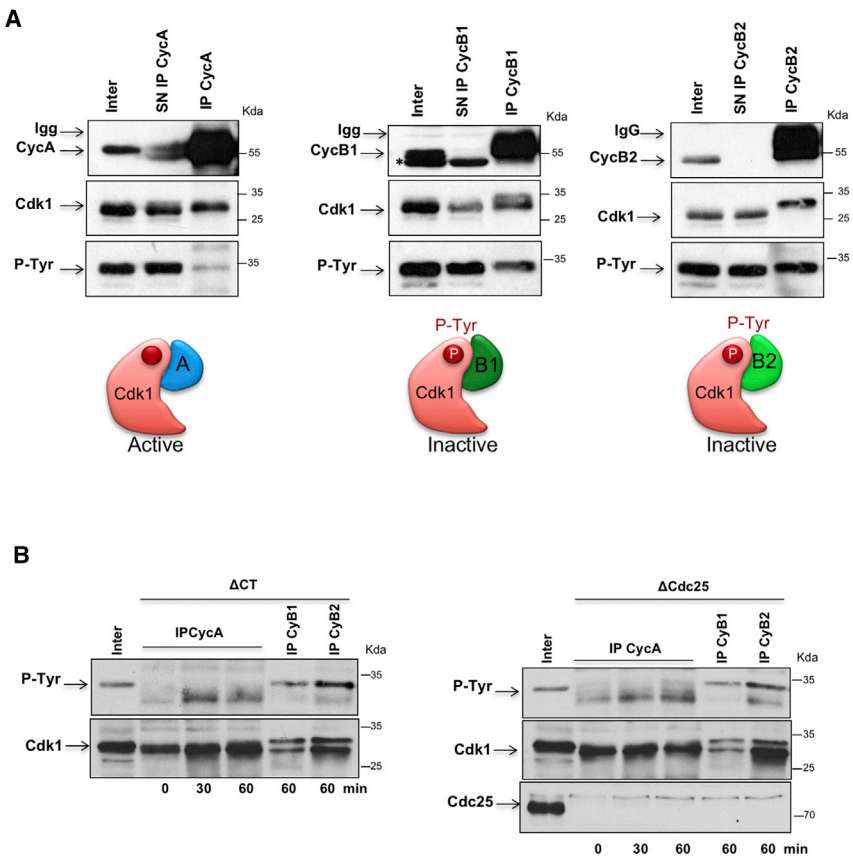

Figure 1. Cyclin A/cdk1-2 Complexes Are Not Phosphorylated on Tyr15 in Interphase *Xenopus* Eggs

(A) Metaphase II oocytes were activated by ionophore treatment and 35 min later lysed and submitted to immunoprecipitation using antibodies against either *Xenopus* cyclin A, cyclin B1, or cyclin B2. Input (Inter), supernatants (SN) and immunoprecipitates (IP) were then analyzed by western blot to assess cyclin A and cdk1 levels as well as phosphorylation of cdk1 on Tyr15 (P-Tyr). A schematic representation of the different cyclin/cdk complexes purified by immunoprecipitation is shown. IgG, immunoglobulins.

(B) *Xenopus* egg extracts prepared as in (A) were depleted with either control (CT) or anti-Cdc25 antibodies. Supernatants were then divided in three aliquots. One of these aliquots was used to immunoprecipitate cyclin A immediately or after 30 and 60 min incubation. The other two aliquots were immunoprecipitated after 60 min incubation with either anti-cyclin B1 or B2 antibodies. Cdk1 and Cdc25 levels, as well as phosphorylation of Tyr15 on cdk1, were monitored.

mitotic substrates of cyclin A/cdk have been identified by phosphoproteomic approaches (Dumitru et al., 2017), the precise mechanism by which cyclin A/cdk could trigger mitotic entry is elusive.

Similarly to cyclin B/cdk1, cyclin A/cdk is submitted to Wee1-inhibitory phosphorylation in human cells, although this phosphorylation is not observed on all cyclin A/cdk complexes (Goldstone et al., 2001; Gu et al., 1992). A recent study reported that a premature activation of cyclin A/cdk upon Wee1 inhibition during G2 in human cells results in an early activation of both Plk1 and cyclin B/cdk1, suggesting that cyclin A/cdk could trigger mitotic entry via Plk1 (Gheghiani et al., 2017). However, it was difficult to discriminate whether Wee1 inhibition promoted mitotic entry through cyclin A/cdk-dependent activation of Plk1 or through dephosphorylation of Tyr15 of cyclin B/cdk1. In this manuscript, we used *Xenopus* egg extracts as a model system that recapitulates mitotic entry with physiological cyclin A and cyclin B levels. These extracts present a high degree of conservation of most essential cellular and molecular mechanisms involved in mitotic entry and progression. Nevertheless, whereas human cells display a partial negative Wee1-dependent phosphorylation of cyclin A/cdk complexes, this negative regulation is not observed in *Xenopus* egg extracts, suggesting that cyclin A/cdk complex formation is immediately followed by the activation of this kinase. We took advantage of this peculiarity (1) to investigate whether progressive accumulation and activation of cyclin A/cdk during G2 could be the triggering factor promoting mitotic entry, and (2) to identify its critical target(s) in this process. We demonstrate that cyclin A-cdk1 phosphorylates Bora on S110 at the G2-M transition, which promotes the phosphorylation of *Xenopus* Plk1 (Plx1) by Aurora A and the full activation of the cyclin B/cdk1 feedback loop. These data define cyclin A/cdk1 as the triggering factor promoting mitotic commitment through the phosphorylation of Bora.

RESULTS

Cyclin A/cdk1-2 Complexes Are Not Phosphorylated on Tyr15 in Interphase *Xenopus* Eggs

Previous observations revealed that cyclin A/cdk1-2 complexes assembled by ectopic addition of cyclin A are not phosphorylated on Tyr15 in *Xenopus* eggs during interphase of the first embryonic division (Clarke et al., 1992). In order to further investigate whether this phosphorylation is also absent on endogenous cyclin A/cdk complexes, we measured phosphorylation of cdk1 on Tyr15 residues on cyclin A, cyclin B1, or cyclin B2 immunoprecipitates (IPs) from interphase egg extracts (35 min post-ionophore treatment, see STAR Methods). As depicted in Figure 1A, we observed a clear Tyr15 phosphorylation on cyclin B1 and B2/cdk1 complexes (middle and right panels) but not on endogenous cyclin A/cdk1-2 (left panel), suggesting that cyclin A/cdk complexes are readily active in interphase.

We next investigated whether the absence of this inhibitory phosphorylation on cyclin A/cdk1-2 could be due to a decreased activity of Wee1/Myt1 kinases or to an increased dephosphorylation activity of Cdc25 toward these complexes. We thus measured Tyr15 phosphorylation on cyclin A IPs at different

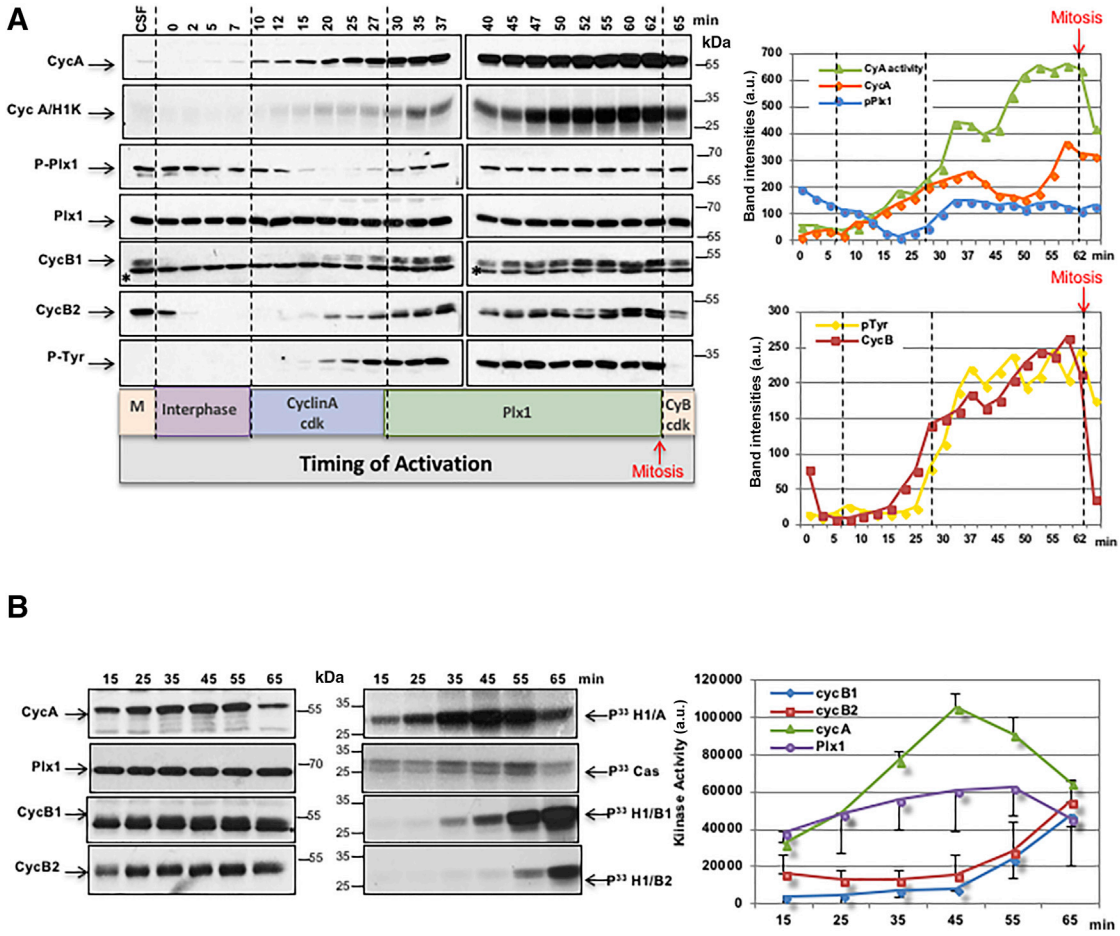

Figure 2. Cyclin A/cdk1 and Plx1 Activities Precede cyclin B/cdk1 Activation and Mitotic Entry in *Xenopus* Eggs

(A) Metaphase II-arrested oocytes were treated with Ca^{2+} ionophore and recovered at the indicated time points. Cyclin A, B1, B2, and Plx1 levels as well as phosphorylation of Plx1 on T201 and of cdk1 on Tyr15 were monitored. Finally, cyclin A/cdk1 activity was also measured in cyclin A immunoprecipitates from two oocytes using histone H1 as a substrate. Band intensities of cyclin A and cyclin B, cyclin A-cdk activity, and phosphorylation of cdk on Tyr15 and of Plx1 on T201 were measured by densitometry using ImageJ.

(B) Cyclin A, B1, B2, and Plx1 immunoprecipitates from two oocytes obtained as in (A) were used to measure kinase activities using histone H1 (for cyclin A/cdk, cyclin B1, and B2/cdk) and casein (for Plx1) as substrates. Autoradiography band intensities were measured by densitometry using ImageJ software in three independent experiments and represented as arbitrary units (a.u.). Mean intensity and standard deviation are represented as in (A). The levels of each of the indicated proteins, as well as the phosphorylation of cdk1 on Tyr15, were also monitored by western blot.

*Denotes non-specific band revealed by anti-cyclin B1 antibodies.

times following Cdc25 depletion. Unlike cyclin B/cdk1 complex, Tyr15 phosphorylation was not observed on cyclin A IPs in these conditions (Figure 1B). These observations strongly suggest that endogenous cyclin A/cdk1-2 is a poor Wee1/Myt1 substrate and that *de novo* formation of cyclin A/cdk1-2 complexes is immediately followed by their activation.

Cyclin A/cdk1-2 and Plx1 Activities Precede Cyclin B/cdk1 Activation and Mitotic Entry in *Xenopus* Eggs

Having determined that cyclin A/cdk complexes are immediately active after their assembly, we monitored the time course of cyclin A/cdk1-2 activation during the first embryonic division of *Xenopus* eggs. We compared this activation with the timing of activation of other key regulators of mitotic entry. Cyclin A protein levels had already started to accumulate 10 min after Ca^{2+} ionophore treatment. This was rapidly followed (2 min later, t = 12 min) by the presence of active cyclin A/cdk1-2 complexes. Remarkably, Plx1 was fully phosphorylated on 20 min after cyclin A/cdk1-2 activation (Figure 2A, t = 30 min). When Plx1, cyclin A/cdk1-2, and cyclin B1/B2/cdk1 activities were specifically measured and compared (Figure 2B), we observed that cyclin A/cdk activity raised from t = 25 to t = 55 and was immediately followed by the activation of Plx1 (from t = 35 to t = 55). Finally, activation of cyclin B1/B2-cdk1 was detectable only from 55 min after Ca^{2+} ionophore treatment.

These observations indicate that endogenous cyclin A/cdk1 activity precedes Plx1 activation, which is followed by cyclin B/cdk activation in *Xenopus* egg progressing into mitosis. These data also suggest that cyclin A/cdk could trigger the cyclin B/cdk activation loop via Plx1.

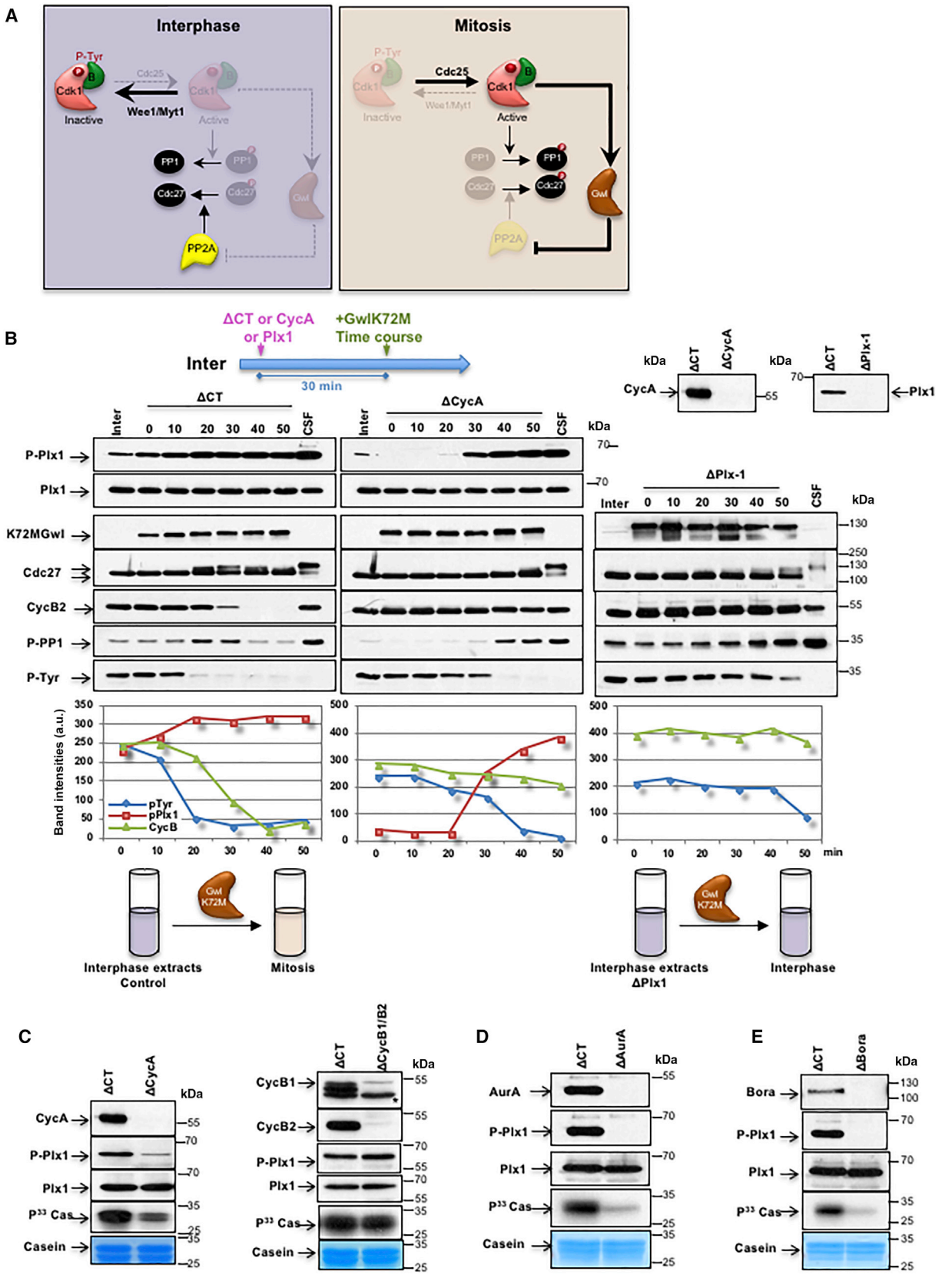

(legend on next page)

Cyclin A/cdk1, through Aurora A/Bora-Dependent Phosphorylation and Activation of Plx1, Is Essential for Mitotic Entry

We next examined whether cyclin A/cdk and Plx1 are essential for mitotic commitment. To this end, we used an experimental setting in which we forced interphase egg extracts to enter into mitosis using low doses of hyperactive Gwl kinase and evaluated the contribution of cyclin A or Plx1 in mitotic entry using immunodepletion experiments.

As shown in Figures 3A and 3B, addition of a low dose of a recombinant hyperactive Gwl kinase (K72MGwl) to interphase extracts partially inhibits PP2A-B55, favors the partial and spontaneous phosphorylation of some cyclin/cdk substrates, and forces mitotic entry. Indeed, addition of hyperactive Gwl resulted by an instantaneous progressive increase of Plx1 activity (Figure 3B, left panel) that was followed 20 min later by the appearance of activated cyclin B/cdk1 and entry into mitosis as indicated by the loss of Tyr15 phosphorylation on cdk and by the phosphorylation of the mitotic substrates Cdc27 and PP1. Thirty minutes post K72MGwl addition, cyclin B levels dropped and extracts exited mitosis concomitantly with the dephosphorylation of the above-mentioned proteins.

If cyclin A/cdk and Plx1 are required for cyclin B/cdk1 activation, the depletion of one of these two kinases before K72MGwl addition might perturb mitotic entry in these extracts. Consistently, cyclin A-depleted extracts displayed a dramatic delay of Plx1 phosphorylation that preceded Tyr15 phosphorylation and activation of cyclin B/cdk1 (Figure 3B, middle panel). In the same line, Plx1 removal (Figure 3B, right panel) fully prevented entry into mitosis, indicating that Plx1 and cyclin A/cdk are both essential for triggering a normal cyclin B/cdk1 activation pattern.

These results prompted us to evaluate whether in *Xenopus* eggs cyclin A/cdk1-2 could induce mitotic division by directly or indirectly promoting Plx1 phosphorylation. We thus measured phosphorylation of Plx1 on the activatory site T201 in interphase extracts that were depleted of cyclin A or B. Cyclin B depletion did not affected Plx1 T201 phosphorylation or activity, whereas the removal of cyclin A induced a dramatic drop of these two parameters (Figure 3C). These data thus confirm that cyclin A/cdk plays an essential role in Plx1 activation. In addition, we could attribute this essential role to the cyclin A/cdk1 complex since the depletion of cdk2 from these extracts did not affect Plx1 phosphorylation or activity (Figure S1A).

We subsequently focused our effort on the identification of the mechanisms involved in Plx1 phosphorylation and activation in interphase extracts. We first investigated whether cyclin A/cdk1 could directly phosphorylate Plx1 on T201. However, a cyclin A/cdk complex immunoprecipitated from interphase extracts was unable to phosphorylate recombinant Plx1 on the activation loop *in vitro* (Figure S1B). We next checked whether Plx1 phosphorylation was promoted by Plkk1 activation, a regulatory kinase previously reported to trigger Plx1 activity in *Xenopus* oocytes (Qian et al., 1998). Again, we did not detect any effect of Plkk1 removal on Plx1 T201 phosphorylation and activity (Figure S1C). Finally, we tested whether Aurora A, whose role in Plk1 activation has been reported in human cells (Macurek et al., 2008; Seki et al., 2008), could be responsible for this phosphorylation. Accordingly, we observed a dephosphorylation of T201 and the complete inactivation of Plx1 when Aurora A was immunodepleted from interphase egg extracts (Figure 3D). We concluded that Plx1 phosphorylation and activation requires Aurora A in *Xenopus* egg extracts.

To further investigate how Aurora A maintains Plx1 activity, we monitored the effect of the removal of the two main cofactors of the Aurora A kinase, the proteins Tpx2 (Eckerdt et al., 2009; Eyers and Maller, 2004) and Bora (Macurek et al., 2008; Seki et al., 2008). Interestingly, whereas Tpx2 elimination did not affect Plx1 phosphorylation or activity (Figure S1D), the removal of Bora was accompanied by the complete dephosphorylation and inactivation of this kinase, suggesting that Plx1 activity in these extracts is maintained by Aurora A and Bora (Figure 3E) in a cyclin A/cdk1-dependent pathway.

Bora Is Essential for Mitotic Commitment in *Xenopus* Egg Extracts

Bora is essential for mitotic entry upon recovery from DNA damage in mammalian cells (Macurek et al., 2008; Seki et al., 2008), but whether it is essential for mitotic entry during an unperturbed cell cycle is unknown. We thus investigated whether Bora is essential for mitotic entry in *Xenopus* egg extracts. Depletion of Bora from interphase extracts prevented Plx1 reactivation, Tyr15 dephosphorylation of cdk1, and mitotic entry after K72MGwl addition (Figure 4A). This phenotype is also observed in cycling extracts in which mitotic division is spontaneously performed (Figure 4B). Moreover, it is specific to Bora removal because mitotic entry was fully rescued when wild-type

Figure 3. Cyclin A/cdk1 Triggers Mitotic Entry via Aurora A/Bora-Dependent Phosphorylation and Activation of Plx1 in *Xenopus* Egg Extracts

(A) Network representing the active (solid arrows) and inactive (dashed arrows) pathways controlling cyclin B/cdk1 and PP2A activities and subsequent protein phosphorylation/dephosphorylation during interphase and mitosis.

(B) 30 μL of interphase extracts were depleted with mock, cyclin A, or Plx1 antibodies, supplemented with cycloheximide at a final concentration of 100 μg/mL and, 30 min later, supplemented again with 250 ng of recombinant GwlK72M hyperactive kinase to force mitotic entry as shown in the scheme. At the indicated times, 1 μL of the mix was used to determine the amount of Plx1, GwlK72M, and cyclin B2 as well as the phosphorylation of Plx1 on T201 (P-Plx1), of Cdc27, of PP1 on threonine 320 (P-PP1), and of Tyr15 of cdk (P-Tyr) by western blot. Cyclin A and Plx1 levels left in the supernatants from control and cyclin A or Plx1 immunoprecipitations are shown. Band intensities of cyclin B levels, phosphorylation of cdk on Tyr15, and of Plx1 on T201 were measured by densitometry using ImageJ. A flowchart describing the experiment is also shown.

(C) Extracts (20 μL) prepared from metaphase II-arrested oocytes 35 min after ionophore treatment were mock or cyclin A or cyclin B1, and cyclin B2 immunodepleted and supplemented with cycloheximide at a final concentration of 100 μg/mL. Part of the supernatant (10 μL) was then used for Plx1 immunoprecipitation to monitor Plx1 kinase activity using casein as a substrate. Coomassie blue staining showing casein amount used in each assay is shown. Cyclin A, cyclin B1, cyclin B2, and Plx1 protein levels as well as phosphorylation of the latter protein on T201 were also monitored by western blot. *Denotes non-specific band of anti-cyclin B1 antibodies.

(D and E) As for (C) except that extracts were immunodepleted using either mock and Aurora A (D) or Bora (E) antibodies.

See also Figure S1.

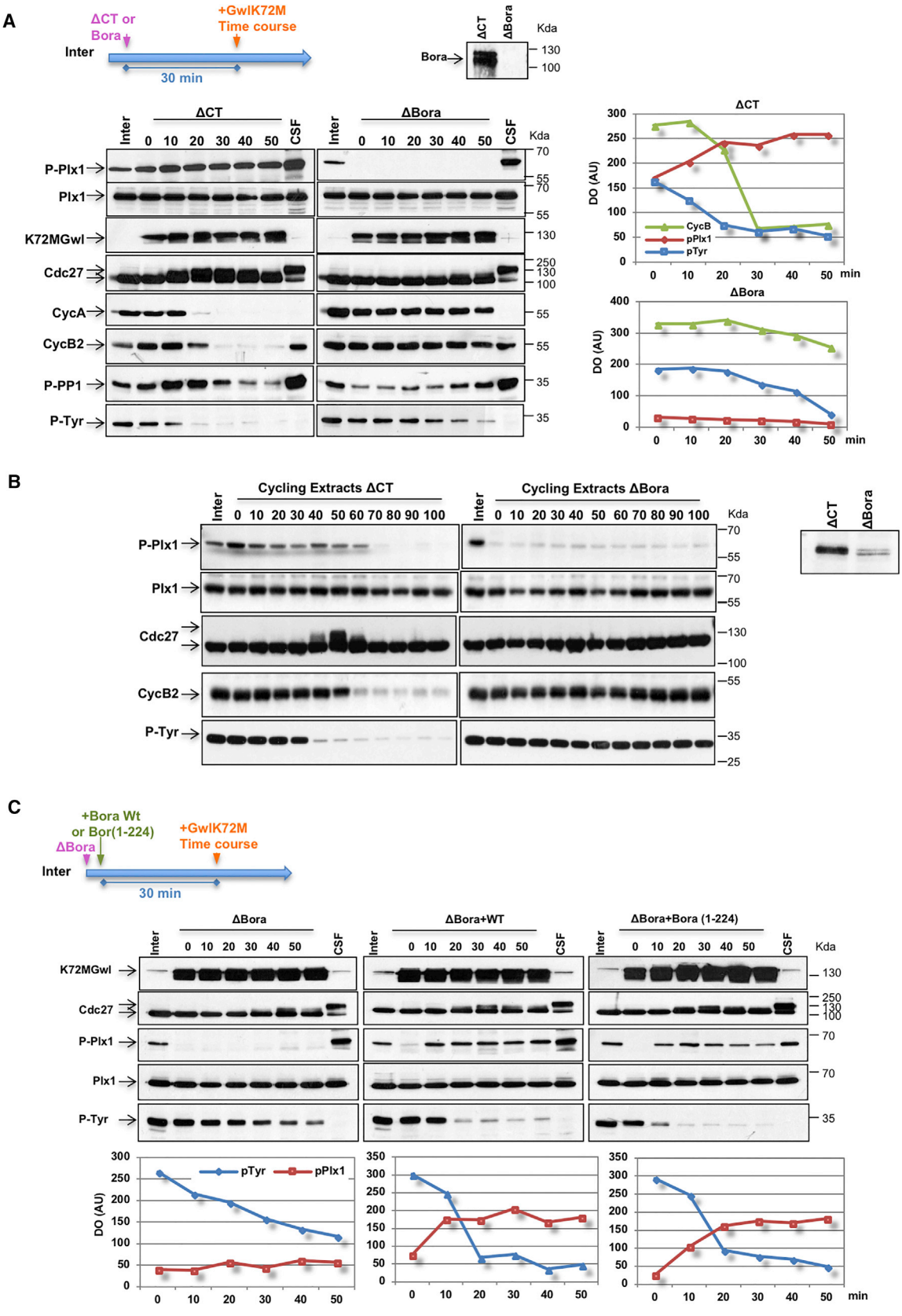

(legend on next page)

full-length *Xenopus* Bora protein was supplemented to Bora-devoid extracts prior to K72MGwl addition (Figure 4C, middle panel). As for full-length Bora, the addition of an N-terminal fragment (Bora 1–224) corresponding to the most conserved part of the protein and previously shown to greatly stimulate Aurora A-dependent phosphorylation of human Plk1 *in vitro* (Thomas et al., 2016) restored mitotic entry in these extracts (Figure 4C, right panel). We concluded that Bora is essential for mitotic entry in *Xenopus* egg extracts.

Cyclin A/cdk1 Promotes Plx1 Activation and Mitotic Entry via the Direct Phosphorylation of Bora on S110

Phosphorylation of human Bora by cyclin B/cdk1 greatly stimulates Aurora A-dependent phosphorylation of Plk1 on T210 *in vitro* (Tavernier et al., 2015; Thomas et al., 2016). We thus sought to determine whether cyclin A/cdk1 induces Plx1 activation by directly phosphorylating Bora. As previously reported for cyclin B/cdk1, we found that cyclin A/cdk1 phosphorylates Bora *in vitro* (Figure 5A). We next investigated whether Bora phosphorylation by cyclin A/cdk1 is required for its function in mitotic entry. To this end, we depleted Bora and its potential activating kinases, cyclin B/cdk1 or cyclin A/cdk1, from interphase extracts and evaluated the capacity of non-phosphorylated Bora to rescue mitotic entry by K72MGwl. Whereas the non-phosphorylated Bora (1–224) fragment readily promoted entry into mitosis in control and cyclin B1-depleted extracts (Figure 5B, left and left-hand middle panel respectively), this form was unable to support entry into mitosis when cyclin A was absent from the extracts (Figure 5B, right-hand middle panel). Consistently, Plx1 and cyclin B/cdk1 kinases were not activated in these extracts. These observations indicate that phosphorylation of exogenous non-phosphorylated Bora by cyclin A/cdk1 is essential in these extracts to promote Plx1 activation and mitotic entry.

We next asked whether we could bypass the need for cyclin A in the extract by providing a version of Bora stably thio-phosphorylated *in vitro* by cyclin A/cdk1. Strikingly, the sole addition to cyclin A-depleted extracts of Bora (1–224) thio-phosphorylated *in vitro* by cyclin A/cdk1, and thus resistant to endogenous phosphatases, completely restored Plx1 phosphorylation and mitotic entry (Figure 5B, right panel). These observations demonstrate that cyclin A/cdk1 induces Plx1 activation through the phosphorylation of Bora. More importantly, these data also demonstrate that, once Bora is fully phosphorylated, cyclin A/cdk is dispensable for mitotic entry under these conditions.

We next focused our efforts in the identification of the residue(s) targeted by cyclin A/cdk1. It has been reported that Bora phosphorylation by cyclin B/cdk1 depends on a conserved cyclin-binding motif at 192LRRKLFLD199/190LRRKLFLD197 (human/*Xenopus*) of Bora. In addition, three conserved cyclin B/cdk1 phosphorylation sites at S41/S38, S112/S110, and S137/S135 (human/*Xenopus* sequence) have been identified as responsible for cdk1-dependent Plk1 activation *in vitro* and *in cellulo* (Tavernier et al., 2015; Thomas et al., 2016). We thus tested whether the cyclin-binding and the cdk phosphorylation sites of *Xenopus* Bora were important for the ability of this protein to promote Plx1 phosphorylation and mitotic entry. Accordingly, deletion of the RXL motif delayed Plx1 activation and mitotic entry in interphase extracts lacking endogenous Bora (Figure 5C, middle panel), while the triple mutation on the conserved cdk phosphorylation sites prevented mitotic commitment (Figure 5C, right panel).

We next investigated the contribution of each of these cdk phosphorylation sites for Bora activity in promoting mitotic entry. To this end, we tested whether individual non-phosphorylatable Bora mutants can rescue mitotic entry in Bora-depleted extracts. While non-phosphorylatable S38A and S135A individual Bora mutants partially restored Plx1 activation and mitotic entry in Bora-depleted extracts (Figure 6A, right and left panels respectively), the Bora S110A mutant was unable to support this event (Figure 6A, middle panel). We concluded that Bora phosphorylation at S110 by cdk is essential for Plx1 activation and mitotic entry.

To gain further mechanistic insight, we developed antibodies specifically recognizing phosphorylated S110 of Bora, and we checked the temporal pattern of phosphorylation upon mitotic entry. As expected, our phospho-S110 Bora antibodies recognized Bora phosphorylated *in vitro* by cyclin A/cdk (Figure 6B). Consistent with our previous observations, the phosphorylation of the cyclin A-cdk site of Bora S110 precedes Plx1 activation and appears long before Tyr15 dephosphorylation of cdk1, supporting cyclin A/cdk1 as the kinase triggering mitotic entry (Figure 6C).

We next asked whether the overexpression of Bora could trigger mitosis in interphase extracts in which the physiological activity of PP2A-B55 was not challenged. With this aim, we monitored S110 phosphorylation of Bora (1–224) as well as Plx1 and cyclin B/cdk1 reactivation in interphase extracts devoid of endogenous Bora, immunodepleted or not of cyclin A and subsequently supplemented with Bora (1–224).

Interestingly, the sole addition of ectopic Bora (1–224) promoted a late but full activation of cyclin B/cdk1 and mitotic entry in control-depleted extracts (Figure 6D, left panel). However, the addition of this protein to cyclin A-depleted interphase extracts abrogated Plx1 T201 and Bora S110 phosphorylations as well

Figure 4. Bora Is Essential for Mitotic Commitment in *Xenopus* Egg Extracts

(A) Interphase extracts were immunodepleted using mock or anti-Bora antibodies and 30 min later supplemented with a recombinant Gwl hyperactive form (GwlK72M) as indicated in the scheme. Samples of 1 μL of extract were recovered at the indicated time points after GwlK72M addition and the levels of Plx1, GwlK72M, cyclin A, cyclin B2, as well as the phosphorylation of Plx1 on T201, Cdc27, PP1 phosphatase on threonine 320 and on Tyr15 of cdk were analyzed by western blot. Band intensities of cyclin B, phosphorylation of Plx1 on T201, and of cdk on Tyr15 were measured by densitometry using ImageJ.

(B) Cycling extracts were mock or Bora depleted and recovered at the indicated time points to measure the levels of Plx1, cyclin B2, and the phosphorylation of Plx1 on T201, of Cdc27, and of cdk1 on Tyr15. The amount of Bora left in the supernatants after immunoprecipitation is shown.

(C) Interphase extracts were depleted of endogenous Bora and supplemented with 250 ng of a Bora wild-type or a C-terminal truncated form of this protein (Bora 1–224). Thirty minutes later, GwlK72M hyperactive kinase was added to force mitotic entry as in the scheme. The levels of GwlK72M and Plx1 and the phosphorylation of Cdc27, of Plx1 on T201, and of cdk on Tyr15 have been assessed. Band intensities of phosphorylation of cdk on Tyr15 and of Plx1 on T201 were measured by densitometry using ImageJ.

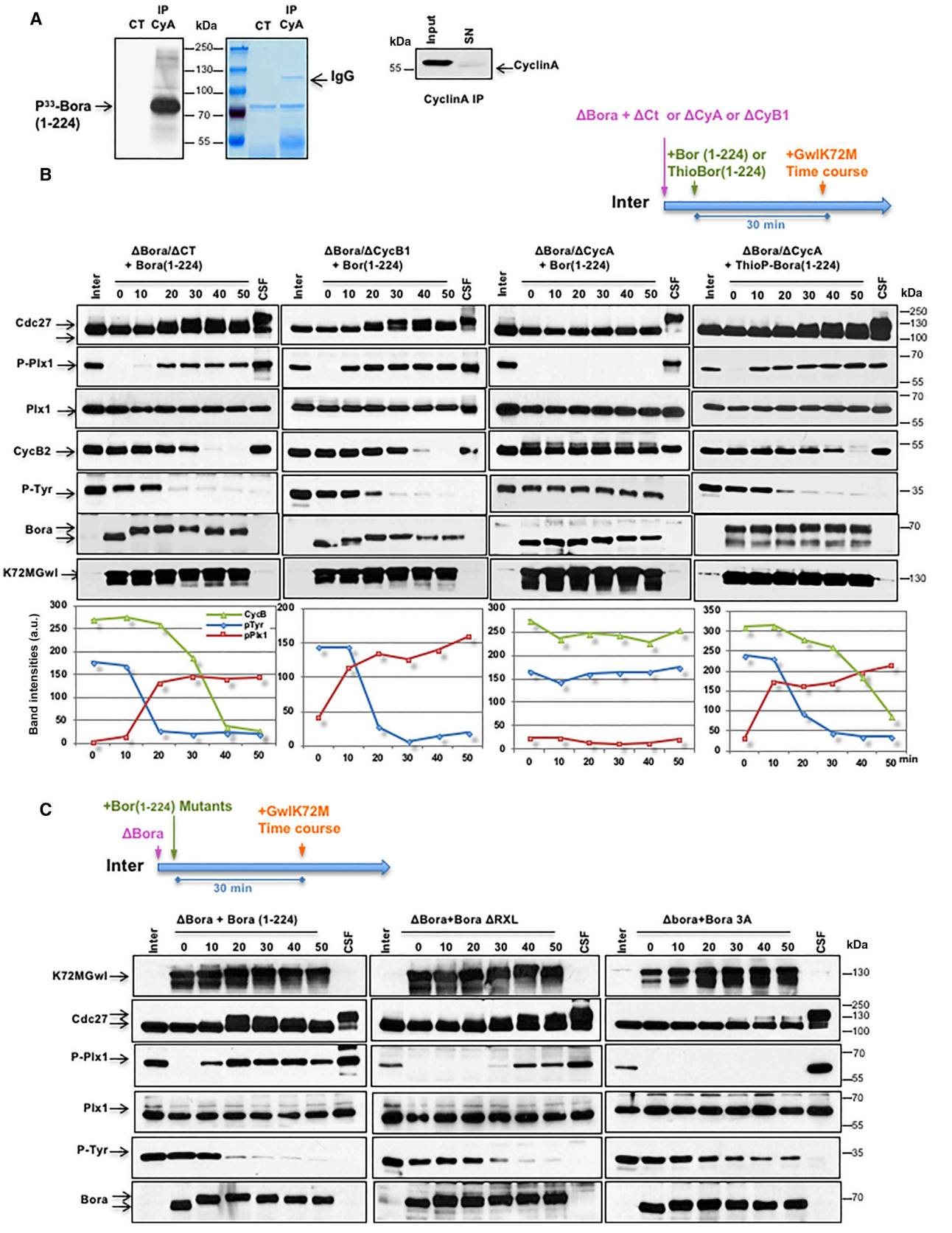

(legend on next page)

as Tyr15 dephosphorylation of cdk1 (Figure 6D, right panel), indicating that the phosphorylation of Bora by cyclin A/cdk1 is the essential event triggering mitotic commitment.

Taken together, these data demonstrate for the first time that cyclin A/cdk1 promotes Aurora A-dependent phosphorylation of Plk1 and mitotic entry through the phosphorylation of Bora on S110.

Construction of a Model for Mitotic Entry Including the Roles of Cyclin A, Bora, and Plx1

To establish the impact of cyclin A/cdk-dependent phosphorylation of Bora on mitotic entry dynamics, we created a mathematical model of the cyclin B/cdk1 regulatory network. Compelling data have previously established that rapid and irreversible mitotic entry results from a bistable switch (Pomerening et al., 2005; Sha et al., 2003). More precisely, the abrupt activity changes of cyclin B/cdk1 activity promoting entry into mitosis is explained as a jump of cell cycle biochemical state at saddle-node bifurcations along the hysteresis response curves due to the activation and inactivation of the cyclin B-cdk1 complex, also named mitotic promoting factor (MPF). The activation of MPF by the MPF activated Cdc25 and MPF inactivated Wee1 and its inactivation by dephosphorylated active Wee1 produce two stable states, also called attractors. Here we denote these attractors by H and L, as they have high and low activity of MPF, respectively. The standard model proposes that the driving force pushing the system from the L to the H attractor is the accumulation of cyclin B during G2 (Hutter et al., 2017; Mochida et al., 2016). We challenged this standard model by taking into account our results demonstrating an essential role of cyclin A, Bora, and Plx1 in triggering MPF activation. Starting from our experimental findings, we first built a mathematical biochemical model for mitotic entry dynamics of the cell cycle (see Methods Details, Mathematical Modeling). The full model includes three dynamical variables, *MPFa*, *MPFi*, and *pPlx1*, which stand for active MPF, inactive MPF, and phosphorylated forms of Plx1, respectively. The time-dependent active cyclin A (*CycAa*) or the phosphorylated form of Bora (*pBora*) are non-autonomous inputs to the full model. When neither *CycAa* nor *pBora* time series are available in the dataset, we considered a partial model made of two dynamical variables, *MPFa* and *MPFi*, with the time-dependent *pPlx1* as input. All the biochemical interactions present in the standard model are also present in our model, with some simplifications. Thus, Wee1 and Cdc25 are represented as functions of *MPFa*. Our model introduces several interactions that are absent in the standard model (Hutter et al., 2017; Mochida et al., 2016). We considered that Plx1 is phosphorylated by Aurora A in the presence of pBora (Macurek et al., 2008; Seki et al., 2008; Tavernier et al., 2015) and dephosphorylated by PP2A (Wang et al., 2015), which is inactivated by *MPFa* (Blake-Hodek et al., 2012). Moreover, we considered that Bora is phosphorylated by *CycAa* (the present work) and that Cdc25 activity depends on both *pPlx1* and *MPFa* (Lindqvist et al., 2009). Furthermore, we supposed that there is a residual activity of Cdc25 in the absence of *MPFa*, whereas there is no activity of Cdc25 in the absence of *pPlx1* (Burgess et al., 2010). For a full description of our model we refer to Methods Details, Mathematical Modeling section. The model parameters were estimated using normalized data from the above experiments (see Methods Details, Mathematical Modeling section and Figure S2). The good agreement between data (Figure S2) and model predictions (Tables S1 and S2) that can be seen in Figure 7A and Figures S3 and S4 supports our modeling choices.

In order to gain further theoretical insight into the mitotic entry phenomenon we used the resulting parametized model to build two types of bifurcation diagrams. In one type of diagram we forced *cycAa*/*pBora* and *cycBtot* to be constant and computed the stable steady states of the full model. In the second type of diagram we performed the same operation for the partial model with imposed values of *pPlx1* and *cycBtot*. The result is shown in Figures 7B and 7C. In both cases we found that, at fixed *pPlx1*, or at fixed *cycAa*/*pBora*, the dependence of *MPFa* on the *cycBtot* has hysteresis. Upon increase of *cycBtot*, the branch of the L attractor loses stability by a saddle-node bifurcation when *cycBtot* exceeds a threshold value *cycBtot** (Figure 7B). At this value, the MPF activity jumps from a low value on the L attractor branch to a high value on the H attractor branch, therefore *cycBtot** corresponds to the mitotic entry. This behavior is identical to the one predicted by the standard model. However, our model includes other predictions. The most important prediction is that *pPlx1 and cycAa*/*pBora* are essential for triggering mitotic entry since, when *pPlx1* and *cycAa*/*pBora* are low, the *cycBtot** threshold increases and becomes infinite (Figure 7C). Moreover, this model also predicts that the levels of *pPlx1* and *cycAa*/*pBora* set up the threshold of *cycBtot* required for mitotic entry and so they establish the length of G2. Accordingly, when *pPlx1* and *cycAa*/*pBora* are increased, the *cycBtot** threshold is lowered and mitotic entry takes place earlier. We tested this prediction by monitoring mitotic entry in cycling extracts in which cyclin B levels were decreased by cyclin B2 immunodepletion and cyclin A concentration was increased by the addition of a low dose of recombinant human cyclin A. Supporting our modeling, upon cyclin A addition, cyclin B2-depleted extracts not only entered into mitosis but this entry was advanced compared with controls

Figure 5. Cyclin A/cdk1 Promotes Plx1 Activation through the Phosphorylation of Bora

(A) Recombinant Bora (1–224) was incubated with phosphorylation buffer alone (CT) or together with a cyclin A/cdk complex obtained by immunoprecipitation of 10 μL of interphase extracts. Shown are autoradiography and Coomassie blue staining. Cyclin A immunodepletion from interphase extracts is also depicted. IgG, immunoglobulins.

(B) Interphase extracts were first devoid of endogenous Bora and subsequently immunodepleted using mock or either cyclin A or cyclin B1 antibodies. Recombinant Bora (1–224) that was *in vitro* thio-phosphorylated or not with a cyclin A/cdk immunoprecipitate was then supplemented. Thirty minutes later, GwlK72M was added to promote entry into mitosis. Levels of Plx1, cyclin B2, Bora, and GwlK72M, as well as phosphorylation of Cdc27, Plx1 in T201, and of cdk on Tyr15, were monitored by western blot at the indicated time points. Band intensities of cyclin B2 levels, phosphorylation of cdk on Tyr15, and of Plx1 on T201 were measured by densitometry using ImageJ.

(C) As for (B) except that Bora (1–224), a Bora (1–224) mutant form of the cyclin-binding motif (ΔRXL), or a triple alanine mutant of cyclin/cdk sites (S38/S110/S135) were added after endogenous Bora depletion.

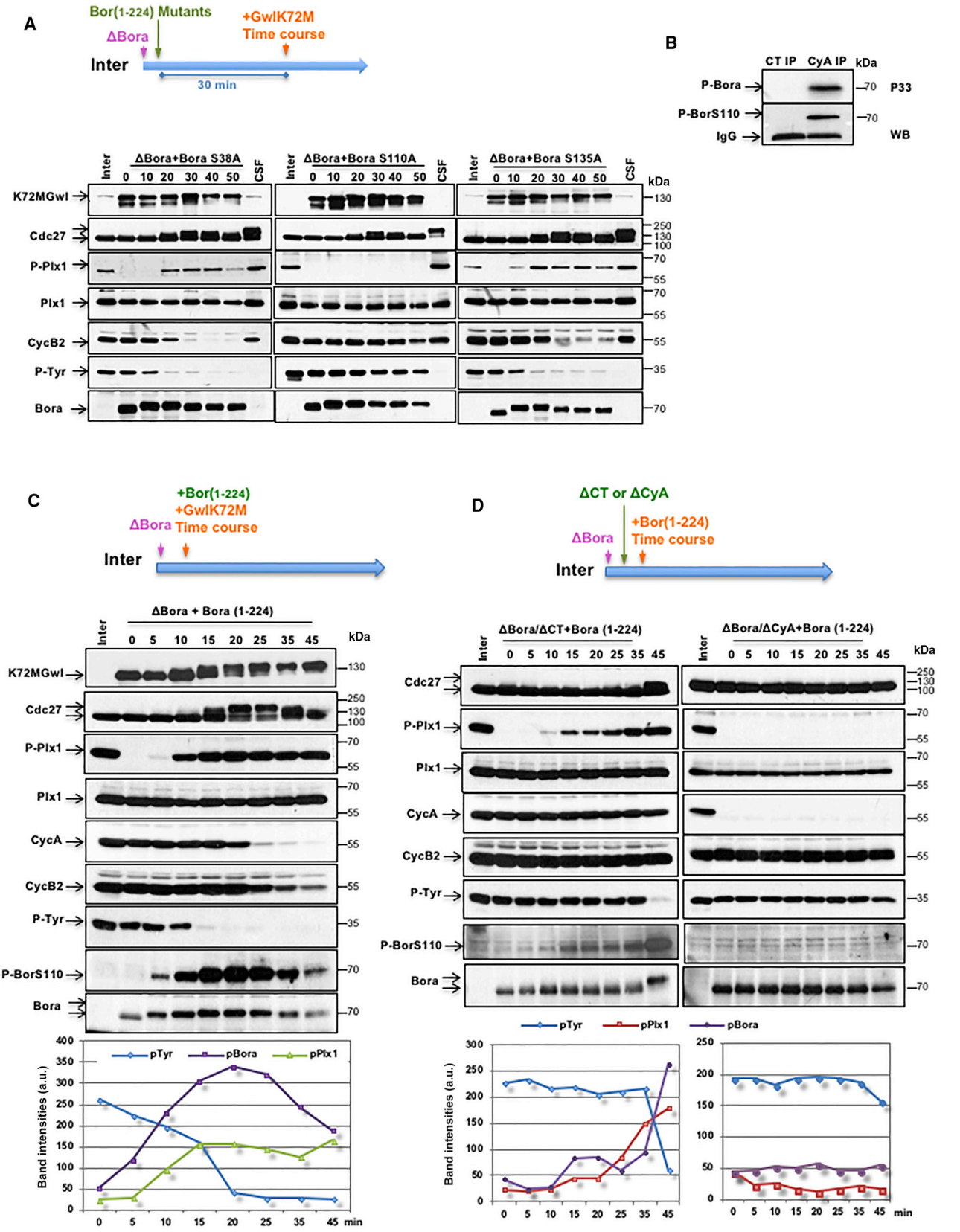

(legend on next page)

(Figure 7D). Another interesting prediction is the all-or-nothing property of the dependence of *cycBtot** on *cycAa/pBora*. Indeed, *cycBtot** is very high and mitotic entry does not take place for low values of *cycAa/pBora*. This prediction was also confirmed by our data showing that the addition of cyclin B to Bora-depleted interphase egg extracts does not promote mitotic entry even when the concentration of this protein was tripled (Figure 7D). Altogether these results show that cyclin A accumulation is the triggering factor that turns on the switch of the bistable state toward a high-MPF mitotic situation.

DISCUSSION

Mitotic entry is an abrupt and irreversible transition that involves the phosphorylation of hundreds of proteins. This massive phosphorylation is the result of the activation of the master kinase cyclin B/cdk1 and the inhibition of the phosphatase PP2A-B55 (Burgess et al., 2010; Gharbi-Ayachi et al., 2010; Mochida et al., 2009; Vigneron et al., 2009). Mitotic entry is triggered by the switch of the Wee1/Myt1-Cdc25 positive feedback loop, which results in the activation of cyclin B/cdk1 and the inhibition of its counteracting phosphatase PP2A-B55. Standard models have assumed that the driving force for mitotic entry is the total level of cyclin B that steadily increases during the G2 phase (Mochida et al., 2016; Tuck et al., 2013). Thus, the length of the G2 phase is set by the amount of cyclin B (Pomerening et al., 2005). This prediction is supported by experimental evidence (Solomon et al., 1990). However, although cyclin B levels contribute to G2 length, it is unlikely that this parameter could trigger cyclin B/cdk1 activation and mitotic entry since, at physiological levels, cyclin B/cdk1 complexes are rapidly inhibited by Wee1/Myt1-dependent phosphorylation soon after formation. As for cyclin B, cyclin A also accumulates during G2. Moreover, when synthesized, cyclin A directly forms active cyclin A/cdk kinase that partially (in human cells) or fully (in *Xenopus* oocytes) escape Wee1/Myt1-inhibitory phosphorylation. These observations point to cyclin A/cdk as the essential factor triggering MPF activation and mitotic entry. Accordingly, we unequivocally demonstrate in this study that cyclin A/cdk1 is the signal triggering mitotic commitment through the phosphorylation of Plx1. Our findings demonstrate that gradual activation of cyclin A/cdk is followed by the increasing activatory phosphorylation of Plx1, which, when reaching a threshold, pulls the bistable switch via the phosphorylation of Cdc25 (Gheghiani et al., 2017). This activation is essential for mitotic entry since Plx1 depletion blocked entry into mitosis even when PP2A-B55 was partially inactivated. More importantly, we could identify the direct substrate of cyclin A/cdk1 responsible for Plx1 activation as the protein Bora. Previous studies reported that Plk1 phosphorylation and activation are mediated in human cells by the kinase Aurora A and require the cofactor Bora (Macurek et al., 2008; Seki et al., 2008). However, although Bora has been recently shown as an essential factor mediating mitotic entry upon DNA damage recovery in mammalian cells (Macurek et al., 2008; Seki et al., 2008), whether it is essential for mitotic entry during an unperturbed cell cycle was not known. Our data clearly demonstrate that cyclin A/cdk1 directly phosphorylates Bora on S110 and that this phosphorylation is necessary and sufficient to promote Plx1 activation and mitotic entry. Accordingly, although cyclin A depletion prevented Plx1 activation and mitosis, this protein is no longer required for Plx1 activation and mitotic commitment if a thio-phosphorylated form of Bora is supplied to interphase extracts.

To establish the impact of cyclin A/cdk1-dependent activation of Bora and Plx1 on the temporal activation of cyclin B/cdk1 and mitotic entry, we generated a mathematical model that includes our observed parameters. Our model brings an important theoretical advance in the comprehension of the mechanisms prompting G2-M transition. Accordingly, and consistent with our data, it predicts that mitotic entry not only requires cyclin B/cdk1 as a driver but also cyclin A/cdk as a trigger for mitotic entry. The role of the trigger would be to lower the threshold value of the driver and in this way to set the length of G2 phase. Another important prediction of this model is that, at levels close to zero of either cyclin A/cdk, pBora, or pPlx1, the amount of cyclin B/cdk required to promote mitotic entry would be infinite. This prediction explains why Bora or Plx1 depletion in *Xenopus* cell-free extracts blocks mitotic entry, establishes cyclin A/cdk activity as the key factor involved in the bistable state switch, and confers the correct timing of mitotic entry.

We propose that during G2, both cyclin B and cyclin A levels accumulate and form cyclin/cdk complexes. Cyclin B/cdk1 is immediately inactivated by phosphorylation by Wee1/Myt1 at Tyr15, whereas cyclin A/cdk escapes, partially (human cells) or completely (*Xenopus* oocytes), inhibitory phosphorylation. This results in the accumulation of active cyclin A/cdk, which, when it reaches a certain activity threshold, promotes the activation of Plx1 via Bora phosphorylation. Active Plx1 then phosphorylates and activates Cdc25 and triggers the cyclin B/cdk1 activation loop and mitotic entry.

In summary, our results identify cyclin A/cdk1 as the signal that turns on the mitotic switch by activating Plx1 through the direct phosphorylation of Bora.

Figure 6. Cyclin A/cdk1 Phosphorylates Bora on S110 and Promotes Plx1 Activation and Mitotic Entry

(A) Interphase extracts were depleted of endogenous Bora; supplemented with a single alanine mutant of each of the three cyclin/cdk sites S38, S110, and S135; and prompted to enter into mitosis by GwlK72M addition. The levels and the phosphorylation of the indicated proteins were monitored by western blot.

(B) Recombinant Bora protein was phosphorylated *in vitro* using a control or a cyclin A IP and analyzed by autoradiography (P33) or by western blot using anti-phospho S110 Bora antibodies (WB). IgG, immunoglobulins.

(C) Interphase extracts were depleted of Bora and re-supplemented with Bora (1–224) and GwlK72M recombinant proteins and at the different time points the levels and the phosphorylation of the indicated proteins assessed by western blot. Band intensities of the phosphorylation of cdk on Tyr15, Bora on S110, and Plx1 on T201 were measured by densitometry using ImageJ.

(D) Bora-depleted interphase extracts were devoid or not of cyclin A, supplemented with Bora (1-224), and the levels and the phosphorylation of the indicated proteins determined. Band intensities of the phosphorylation of cdk on Tyr15, of Plx1 on T201, and of Bora on S110 were measured by densitometry using ImageJ.

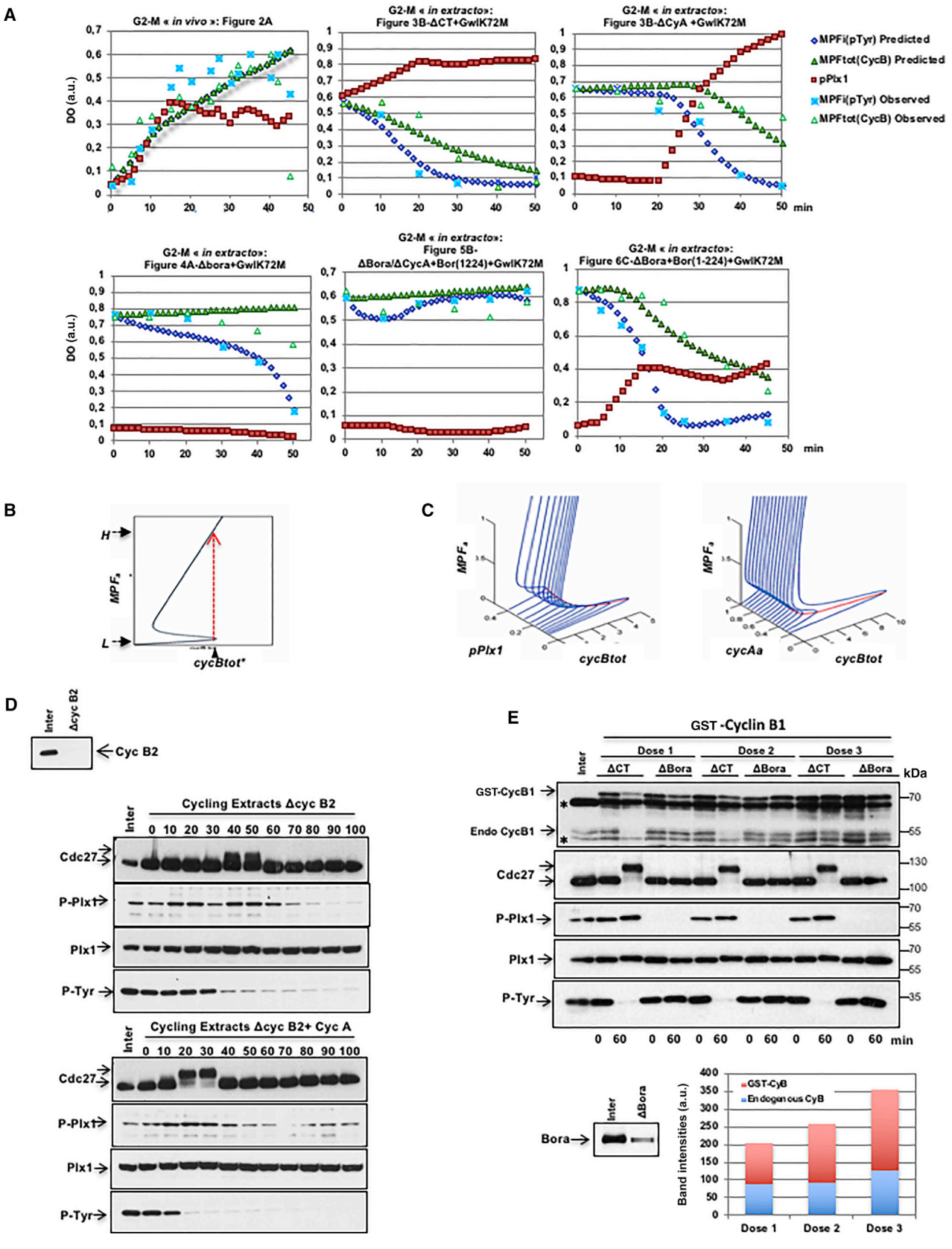

(legend on next page)

STAR★METHODS

Detailed methods are provided in the online version of this paper and include the following:

- KEY RESOURCES TABLE
- CONTACT FOR REAGENT AND RESOURCE SHARING
- EXPERIMENTAL MODEL AND SUBJECT DETAILS
  - *Xenopus laevis* Induction and Husbandry
- METHOD DETAILS
  - Interphase, Cycling and CSF Xenopus Egg Extracts
  - Immunoprecipitation
  - Casein and H1 Kinase Activities
  - *In Vitro* Phosphorylation
  - Thio-Phosphorylation of Xenopus Bora (1-224)
  - Plasmids, Antibodies and Immunoblots
  - Antibody Production and Purification
  - Site-Directed Mutagenesis
  - Purification of Human Cyclin A
  - Mathematical Modelling
- QUANTIFICATION AND STATISTICAL ANALYSIS
- DATA AND SOFTWARE AVAILABILITY

SUPPLEMENTAL INFORMATION

Supplemental Information includes four figures and two tables and can be found with this article online at https://doi.org/10.1016/j.devcel.2018.05.005.

ACKNOWLEDGMENTS

We thank Dr. N. Morin for the generous gift of the anti-Tpx2 antibodies. We also thank P. Richard and M. Plays from the Antibody Production Platform at the CRBM. We thank A. Dupuis for valuable help in some key experiments. This work was supported by the Agence Nationale de la Recherche (ANR-17-CE13-0011-01/02), the Fondation pour la Recherche Médicale (FRM) grant number DEQ20150331692 to A.C., and the Labex EpiGenMed (ANR-10-LABEX-12-01). L.S. has a Labex EpiGenMed and a Ligue National Contre le Cancer program fellowship.

AUTHOR CONTRIBUTIONS

S.V. designed experiments, performed most experiments, and analyzed data. L.S. performed biochemical experiments in activated oocytes. J.-C.L. helped with the biochemical purifications. L.P. participated in discussions and experimental design. O.R. performed mathematical modeling and wrote the corresponding parts of the paper. A.C. analyzed data and wrote the paper. T.L. designed experiments, analyzed data, and wrote the paper.

DECLARATION OF INTERESTS

The authors declare no competing financial interests.

Received: January 30, 2018
Revised: April 4, 2018
Accepted: May 2, 2018
Published: June 4, 2018

REFERENCES

Abrieu, A., Doree, M., and Picard, A. (1997). Mitogen-activated protein kinase activation down-regulates a mechanism that inactivates cyclin B-cdc2 kinase in G2-arrested oocytes. Mol. Biol. Cell *8*, 249–261.

Blake-Hodek, K.A., Williams, B.C., Zhao, Y., Castilho, P.V., Chen, W., Mao, Y., Yamamoto, T.M., and Goldberg, M.L. (2012). Determinants for activation of the atypical AGC kinase Greatwall during M phase entry. Mol. Cell. Biol. *32*, 1337–1353.

Burgess, A., Vigneron, S., Brioudes, E., Labbe, J.C., Lorca, T., and Castro, A. (2010). Loss of human Greatwall results in G2 arrest and multiple mitotic defects due to deregulation of the cyclin B-Cdc2/PP2A balance. Proc. Natl. Acad. Sci. USA *107*, 12564–12569.

Castro, A., Bernis, C., Vigneron, S., Labbe, J.C., and Lorca, T. (2005). The anaphase-promoting complex: a key factor in the regulation of cell cycle. Oncogene *24*, 314–325.

Chan, E.H., Santamaria, A., Sillje, H.H., and Nigg, E.A. (2008). Plk1 regulates mitotic Aurora A function through betaTrCP-dependent degradation of hBora. Chromosoma *117*, 457–469.

Clarke, P.R., Leiss, D., Pagano, M., and Karsenti, E. (1992). Cyclin A- and cyclin B-dependent protein kinases are regulated by different mechanisms in *Xenopus* egg extracts. EMBO J. *11*, 1751–1761.

Deibler, R.W., and Kirschner, M.W. (2010). Quantitative reconstitution of mitotic CDK1 activation in somatic cell extracts. Mol. Cell *37*, 753–767.

Dumitru, A.M.G., Rusin, S.F., Clark, A.E.M., Kettenbach, A.N., and Compton, D.A. (2017). Cyclin A/Cdk1 modulates Plk1 activity in prometaphase to regulate kinetochore-microtubule attachment stability. eLife *6*, e29303.

Eckerdt, F., Pascreau, G., Phistry, M., Lewellyn, A.L., DePaoli-Roach, A.A., and Maller, J.L. (2009). Phosphorylation of TPX2 by Plx1 enhances activation of Aurora A. Cell Cycle *8*, 2413–2419.

Eyers, P.A., and Maller, J.L. (2004). Regulation of *Xenopus* Aurora A activation by TPX2. J. Biol. Chem. *279*, 9008–9015.

Gharbi-Ayachi, A., Labbe, J.C., Burgess, A., Vigneron, S., Strub, J.M., Brioudes, E., Van-Dorsselaer, A., Castro, A., and Lorca, T. (2010). The substrate of Greatwall kinase, Arpp19, controls mitosis by inhibiting protein phosphatase 2A. Science *330*, 1673–1677.

Gheghiani, L., Loew, D., Lombard, B., Mansfeld, J., and Gavet, O. (2017). PLK1 activation in late G2 sets up commitment to mitosis. Cell Rep. *19*, 2060–2073.

Figure 7. Construction of a Model for Mitotic Entry Including the Roles of Cyclin A, Bora, and Plx1

(A) Data/prediction comparison using *pPlx1* input. Time series were predicted by our model with optimal parameters. Predicted and observed data are indicated. *pPlx1* time series is piecewise cubic interpolated from data.

(B) Hysteresis curves during the G2/M transition. H and L are branches of attractors with high and low activity of MPF. Mitotic entry occurs when the total amount of cyclin B reaches the saddle-node bifurcation value *cycBtot** and the MPF activity increases discontinuously by a jump from L to H.

(C) In our model the threshold *cycBtot** depends on *p-Plx1* (left) or active cyclin A amounts (right). This dependence is shown by a red line in the three-dimensional plots. A high *cycBtot** value means a retarded mitotic entry. For vanishing values of *p-Plx1*, or equivalently for vanishing values of cycA active/pBora, the threshold *cycBtot** is so high that mitotic entry is hindered. Changing the amount of cycA active/pBora or p-Plx1 modifies the timing of mitotic entry and the length of G2 phase. See also Figures S2–S4 and Tables S1 and S2.

(D) Cycling extracts were depleted of cyclin B2 antibodies and supplemented or not with recombinant human Cyclin A protein (final concentration: 3.3 ng/μL). An aliquot of 1 μL of each mix was used to monitor mitotic entry at the indicated time points by checking the levels and the phosphorylation of Cdc27, Plx1 on T201, and cdk1 on Tyr15. Levels of cyclin B2 left in the supernatants are shown.

(E) Interphase extracts were depleted (ΔBora) or not (ΔCT) of Bora and supplemented with increasing doses of recombinant glutathione S-transferase (GST)-cyclin B. The levels of ectopic and endogenous cyclin B1 and of Plx1 and the phosphorylation of Cdc27, Plx1 on T201, and of cdk1 on Tyr15 were measured by western blot. Bora amount left in the supernatants of Bora immunoprecipitation is shown. The levels of ectopic and recombinant cyclin B1 in the extracts were measured by densitometry using ImageJ. *Denotes non-specific bands of anti-cyclin B1 antibody.

Goldstone, S., Pavey, S., Forrest, A., Sinnamon, J., and Gabrielli, B. (2001). Cdc25-dependent activation of cyclin A/cdk2 is blocked in G2 phase arrested cells independently of ATM/ATR. Oncogene *20*, 921–932.

Gu, Y., Rosenblatt, J., and Morgan, D.O. (1992). Cell cycle regulation of CDK2 activity by phosphorylation of Thr160 and Tyr15. EMBO J. *11*, 3995–4005.

Hutter, L.H., Rata, S., Hochegger, H., and Novak, B. (2017). Interlinked bistable mechanisms generate robust mitotic transitions. Cell Cycle *16*, 1885–1892.

Jang, Y.J., Ma, S., Terada, Y., and Erikson, R.L. (2002). Phosphorylation of threonine 210 and the role of serine 137 in the regulation of mammalian polo-like kinase. J. Biol. Chem. *277*, 44115–44120.

Lane, H.A., and Nigg, E.A. (1996). Antibody microinjection reveals an essential role for human polo-like kinase 1 (Plk1) in the functional maturation of mitotic centrosomes. J. Cell Biol. *135*, 1701–1713.

Lindqvist, A., Rodriguez-Bravo, V., and Medema, R.H. (2009). The decision to enter mitosis: feedback and redundancy in the mitotic entry network. J. Cell Biol. *185*, 193–202.

Lobjois, V., Froment, C., Braud, E., Grimal, F., Burlet-Schiltz, O., Ducommun, B., and Bouche, J.P. (2011). Study of the docking-dependent PLK1 phosphorylation of the CDC25B phosphatase. Biochem. Biophys. Res. Commun. *410*, 87–90.

Lorca, T., Bernis, C., Vigneron, S., Burgess, A., Brioudes, E., Labbe, J.C., and Castro, A. (2010). Constant regulation of both the MPF amplification loop and the Greatwall-PP2A pathway is required for metaphase II arrest and correct entry into the first embryonic cell cycle. J. Cell Sci. *123*, 2281–2291.

Lorca, T., Castro, A., Martinez, A.M., Vigneron, S., Morin, N., Sigrist, S., Lehner, C., Doree, M., and Labbe, J.C. (1998). Fizzy is required for activation of the APC/cyclosome in *Xenopus* egg extracts. EMBO J. *17*, 3565–3575.

Macurek, L., Lindqvist, A., Lim, D., Lampson, M.A., Klompmaker, R., Freire, R., Clouin, C., Taylor, S.S., Yaffe, M.B., and Medema, R.H. (2008). Polo-like kinase-1 is activated by aurora A to promote checkpoint recovery. Nature *455*, 119–123.

Mochida, S., Ikeo, S., Gannon, J., and Hunt, T. (2009). Regulated activity of PP2A-B55 delta is crucial for controlling entry into and exit from mitosis in *Xenopus* egg extracts. EMBO J. *28*, 2777–2785.

Mochida, S., Rata, S., Hino, H., Nagai, T., and Novak, B. (2016). Two bistable switches govern M phase entry. Curr. Biol. *26*, 3361–3367.

Nakajima, H., Toyoshima-Morimoto, F., Taniguchi, E., and Nishida, E. (2003). Identification of a consensus motif for Plk (Polo-like kinase) phosphorylation reveals Myt1 as a Plk1 substrate. J. Biol. Chem. *278*, 25277–25280.

Pagano, M., Pepperkok, R., Verde, F., Ansorge, W., and Draetta, G. (1992). Cyclin A is required at two points in the human cell cycle. EMBO J. *11*, 961–971.

Pomerening, J.R., Kim, S.Y., and Ferrell, J.E., Jr. (2005). Systems-level dissection of the cell-cycle oscillator: bypassing positive feedback produces damped oscillations. Cell *122*, 565–578.

Qian, Y.W., Erikson, E., and Maller, J.L. (1998). Purification and cloning of a protein kinase that phosphorylates and activates the polo-like kinase Plx1. Science *282*, 1701–1704.

Roshak, A.K., Capper, E.A., Imburgia, C., Fornwald, J., Scott, G., and Marshall, L.A. (2000). The human polo-like kinase, PLK, regulates cdc2/cyclin B through phosphorylation and activation of the cdc25C phosphatase. Cell. Signal. *12*, 405–411.

Seki, A., Coppinger, J.A., Jang, C.Y., Yates, J.R., and Fang, G. (2008). Bora and the kinase Aurora a cooperatively activate the kinase Plk1 and control mitotic entry. Science *320*, 1655–1658.

Sha, W., Moore, J., Chen, K., Lassaletta, A.D., Yi, C.S., Tyson, J.J., and Sible, J.C. (2003). Hysteresis drives cell-cycle transitions in *Xenopus laevis* egg extracts. Proc. Natl. Acad. Sci. USA *100*, 975–980.

Solomon, M.J., Glotzer, M., Lee, T.H., Philippe, M., and Kirschner, M.W. (1990). Cyclin activation of p34cdc2. Cell *63*, 1013–1024.

Tavernier, N., Noatynska, A., Panbianco, C., Martino, L., Van Hove, L., Schwager, F., Leger, T., Gotta, M., and Pintard, L. (2015). Cdk1 phosphorylates SPAT-1/Bora to trigger PLK-1 activation and drive mitotic entry in *C. elegans* embryos. J. Cell Biol. *208*, 661–669.

Thomas, Y., Cirillo, L., Panbianco, C., Martino, L., Tavernier, N., Schwager, F., Van Hove, L., Joly, N., Santamaria, A., Pintard, L., et al. (2016). Cdk1 phosphorylates SPAT-1/Bora to promote Plk1 activation in *C. elegans* and human cells. Cell Rep. *15*, 510–518.

Tsai, T.Y., Theriot, J.A., and Ferrell, J.E., Jr. (2014). Changes in oscillatory dynamics in the cell cycle of early *Xenopus laevis* embryos. PLoS Biol. *12*, e1001788.

Tuck, C., Zhang, T., Potapova, T., Malumbres, M., and Novak, B. (2013). Robust mitotic entry is ensured by a latching switch. Biol. Open *2*, 924–931.

Vigneron, S., Brioudes, E., Burgess, A., Labbe, J.C., Lorca, T., and Castro, A. (2009). Greatwall maintains mitosis through regulation of PP2A. EMBO J. *28*, 2786–2793.

Vigneron, S., Gharbi-Ayachi, A., Raymond, A.A., Burgess, A., Labbe, J.C., Labesse, G., Monsarrat, B., Lorca, T., and Castro, A. (2011). Characterization of the mechanisms controlling Greatwall activity. Mol. Cell. Biol *31*, 2262–2275.

Wang, L., Guo, Q., Fisher, L.A., Liu, D., and Peng, A. (2015). Regulation of polo-like kinase 1 by DNA damage and PP2A/B55alpha. Cell Cycle *14*, 157–166.

Watanabe, N., Arai, H., Iwasaki, J., Shiina, M., Ogata, K., Hunter, T., and Osada, H. (2005). Cyclin-dependent kinase (CDK) phosphorylation destabilizes somatic Wee1 via multiple pathways. Proc. Natl. Acad. Sci. USA *102*, 11663–11668.

Woo, R.A., and Poon, R.Y. (2003). Cyclin-dependent kinases and S phase control in mammalian cells. Cell Cycle *2*, 316–324.

STAR★METHODS

KEY RESOURCES TABLE

REAGENT or RESOURCE	SOURCE	IDENTIFIER
Antibodies		
Rabbit Polyclonal anti-Human Greatwall	Burgess et al., 2010	N/A
Rabbit Polyclonal anti-Xenopus Cdc27	Lorca et al., 2010	N/A
Rabbit Polyclonal anti-Xenopus Cdc25	Lorca et al., 2010	N/A
Rabbit Polyclonal Phospho-Cdc2 (Tyr-15)	Cell Signalling Technology	Cat#9111; RRID:AB_2074655
Rabbit Polyclonal anti-Xenopus Cyclin B2	Abrieu et al., 1997	N/A
Rabbit Polyclonal anti-Xenopus Cdk1	This study	N/A
Rabbit Monoclonal PhosphoThr320 of PP1	Abcam	Cat#62334; RRID:AB_956236
Rabbit Polyclonal anti-Xenopus Tpx2	Dr N Morin (CRBM-CNRS, Montpellier, France)	N/A
Rabbit Polyclonal anti-Xenopus Cyclin A1	Lorca et al., 2010	N/A
Rabbit Polyclonal anti-Xenopus Cdk2	This study	N/A
Rabbit Polyclonal anti-Xenopus Bora	This sutdy	N/A
Rabbit Polyclonal anti-Xenopus N-ter Bora	This study	N/A
Rabbit Polyclonal anti-S110 Bora	This study	N/A
Rabbit Polyclonal anti-Xenopus Plx1	This study	N/A
Rabbit Polyclonal phospho-Human T210 Plk1	Cell Signalling Technology	Cat#9062; RRID:AB_11127447
Rabbit Polyclonal anti-Xenopus Plkk	This study	N/A
Rabbit Polyclonal anti-Xenopus Cyclin B1	This study	N/A
HRP conjugated anti-Rabbit secondary antibodies	Cell Signalling Technology	Cat#7074; RRID:AB_2099233
HRP conjugated anti-Mouse secondary antibodies	BioRad	Cat#1172-1011; RRID:AB_2617113
Rabbit Polyclonal anti-GST antibodies	This study	N/A
Bacterial and Virus Strains		
BL21DE3 Competent E.Coli	New England Biolabs	Cat#C2527H
DH5α E. Coli	New England Biolabs	Cat#C2987I
Chemicals, Peptides, and Recombinant Proteins		
ATP gamma p33	Perkin Elmer	Cat#NEG602H1001MC
Peptide for Xenopus Cdk2 antibodies: FRDVSRPTPHLI	Proteogenix	N/A
Peptide for Xenopus Nter Bora antibodies: MGDVRTQLTPET	Proteogenix	N/A
Peptide for Phospho-110 Bora antibodies: CRTIVPS(PO_3H_2)PWTQHE-COOH	Proxeogenix	N/A
HCG Hormone	Intervet-MSD Sante Animal	Cat#6968493
Pfu ultra II fusion DNA polymerase	Agilent	Cat#600670
$ATP^{\gamma S}$	Sigma	Cat#A1388
Calcium Ionophore	Sigma	Cat#A231987
Dynabeads protein G	Invitrogen	Cat#1009D
Okadaic Acid	Life Technologies	Cat#13166-012
Histone H1	Sigma	Cat#14-155
Casein	Sigma	Cat#C7078
Thyroglobulin from bovine thyroid	Sigma	Cat#T1001
BSA	Sigma	Cat#A7906
Glutathione Sepharose™ hFastFlow	GE Healthcare	Cat#17-5132-02
CNBr-activated sepharose 4B	GE Healthcare	Cat#17-0430-01
Amylose Resin High Flow	Biolabs	Cat#E80225
Sulfo-MBS	Thermo Scientific	Cat#22312

(*Continued on next page*)

Continued

REAGENT or RESOURCE	SOURCE	IDENTIFIER
Recombinant GST-Human Greatwall K72M mutant	Vigneron et al., 2011	N/A
Recombinant Human Cyclin A protein	This study	N/A
RecA-HRP	Life Technologies	Cat#101123
Experimental Models: Organisms/Strains		
Xenopus Laevis	Centre de Ressources Biologiques Xenopes-Rennes	http://www.celphedia.eu/en/centers/crb
Oligonucleotides		
Forward and reverse primers for BoraΔRXL deletion: 5' CAG-CTC-CTC-CTC-CCT-TAG-ATT-TTT-GGA-TGG-TCA-TGC-C 3' 5' GGC-ATG-ACC-ATC-CAA-AAA-TCT-AAG-GGA-GGA-GGA-GCT-G 3'	Eurogentec	This study
Forward and reverse primers for Bora S38A: 5' CAT-GAG-CCA-TTT-GTT-TCT-GCC-CCA-TCT-GTA-TTC-AAG-CC 3' 5' GGC-TTG-AAT-ACA-GAT-GGG-GCA-GAA-ACA-AAT-GGC-TCA-TG 3'	Eurogentec	This study
Forward and reverse primers for Bora S110A: 5' GAG-AAC-AAT-TGT-TCC-AGC-ACC-ATG-GAC-TCA-ACA-CG 3' 5' CGT-GTT-GAG-TCC-ATG-GTG-CTG-GAA-CAA-TTG-TTC-TC 3'	Eurogentec	This study
Forward and reverse primers for BoraS135A: 5' GCC-GAT-CTT-ATT-CAT-GAA-GCC-CCT-GTA-GGG-AGA-G 3' 5' CTC-TCC-CTA-CAG-GGG-CTT-CAT-GAA-TAA-GAT-CGG-C 3'	Eurogentec	This study
Cloning Xenopus Bora into pGEX4T1 ; forward and reverse primers: 5'TCG-GGG-AAT-TCA-TGG-GTG-ATG-TGC-GTA-CCC3' 5' TGC-CAG-CGG-CCG-CTT-ACT-GCA-GGA-AAT-GTG-ACA-AG 3'	Eurogentec	This study
Cloning Xenopus Bora into pMalP2 ; forward and reverse primers: 5'TCG-GGG-AAT-TCA-TGG-GTG-ATG-TGC-GTA-CCC3' 5'CAC-GGA-AGC-TTT-TAC-TGC-AGG-AAA-TGT-GAC-AAG 3'	Eurogentec	This study
Cloning Xenopus Bora (1-224) into pMalC2x ; forward and reverse primers : 5'CCT-GCG-GAT-CCA-TGG-GTG-ATG-TGC-GTA-CCC3' 5'CCG-CCG-TCG-ACT-TAC-TGC-AGG-AAA-TGT-GAC-AAG 3'	Eurogentec	This study
Cloning Xenopus Plkk into pGEX4T1; forward and reverse primers: 5' GAC-GGC-GAA-TTC-ATG-GCT-TTC-GCC-AAC-TTC-CGC 3' 5' GCC-AGC-CTC-GAG-GCC-AGA-ATC-GGA-ATC-CCT 3'	Eurogentec	This study
Amplification of Xenopus Bora from Xenopus ovary cDNA; forward and reverse primers: 5' ATGGGTGATGTGCGTACCC 3' 5' TTACTGCAGGAAATGTGACAAG 3'	Eurogentec	This study
Recombinant DNA		
pGEX4T1 Bora Xenopus	This study	N/A
pGEX4T1Plkk Xenoppus	This study	N/A
pCR4Topo Plkk Xenopus	Biovalley	Cat#IRBJp5024M135Q
pGEX 4TCdk2	Dr J Gauthier (Columbia University, New York,USA)	N/A
pMalP2Bora Xenopus	This study	N/A
pMalC2x Bora Xenopus (1-224)	This study	N/A
pCS2 Bora Xenopus	This study	N/A
pT7F1-Human cyclin A	Dr G Draetta (University of Texas, US)	N/A
Software and Algorithms		
Adobe Photoshop	Microsoft	Version 12.0x64
Excel	Microsoft	Version 14.7.7
PowerPoint	Microsoft	Version 14.7.7
ImageJ	NIH	1.50i

(*Continued on next page*)

Continued

REAGENT or RESOURCE	SOURCE	IDENTIFIER
Optimization Toolbox Release	The MathWorks Inc	https://fr.mathworks.com/products/optimization.html
MATLAB	The MathWorks Inc	https://fr.mathworks.com/products/matlab.html?s_tid=hp_products_matlab

CONTACT FOR REAGENT AND RESOURCE SHARING

Further information and requests for resources and reagents should be directed to and will be fulfilled by the Lead Contact, Thierry Lorca (thierry.lorca@crbm.cnrs.fr).

EXPERIMENTAL MODEL AND SUBJECT DETAILS

Xenopus laevis Induction and Husbandry

Regulations for the use of *Xenopus laevis*, as outlined in the Animals Scientific Procedures Act (ASPA) and implemented by the Direction Generale de la Recherche et Innovation, Ministère de L'Enseignement Supérieur de l'Innovation of France were followed.

Frogs were obtained from « Centre de Ressources Biologiques Xénopes (CRB) of Rennes», France and kept in a *Xenopus* research facility at the CRBM (Facility Center approved by the French Gouverment. Approval n° B34-172-39).

Females were injected of 500 U Chorulon (Human Chorionic Gonadotrophin) and oocytes layed 18h later were used for experiments. Adult females were exclusively used to obtain eggs. All procedures were approved by the ''Direction Generale de la Recherche et l'Innovation'', Ministère de L'Enseignement Supérieur de l'Innovation of France (Approval n° APAFIS#4971-2016041415177715v4).

METHOD DETAILS

Interphase, Cycling and CSF Xenopus Egg Extracts

Interphase Xenopus egg extracts obtained from metaphase II-arrested oocytes 35 minutes after Ca^{2+} Ionophore (final concentration 2 μg/ml) treatment. Metaphase II-arrested egg extracts also named Cytostatic Factor (CSF)-arrested eggs were obtained by crushing metaphase II-arrested oocytes in the presence of EGTA at a final concentration of 5mM (Lorca et al., 2010). Cycling extracts were obtained as interphase extracts except that they were recovered 50 minutes after Ca^{2+} Ionophore and used freshly.

For Figure 2, dejellied metaphase II-arrested oocytes were activated by Ca^{2+} Ionophore (final concentration of 2 μg/μl) and at the indicated time-points removed in groups of two and directly frozen at -80°C. When used, oocytes were thawed and homogenized in 60 μl of buffer containing 80 mM βGlycerophosphate, 20 mM EGTA, 15 mM $MgCl_2$ pH7.3, centrifuged for 5 minutes at 10 000 g and supplemented with 20 μl of Laemmli-SDS buffer. 30 μl of this sample was loaded in a 10% polyacrylamide gel.

Immunoprecipitation

Immunoprecipitations were carried out for 20 minutes at room temperature using 2 μg of affinity-purified antibodies immobilized on 20 μl protein G-Dynabeads (Dynal) and 20 μl of Xenopus egg extracts. When supernatant was used, beads were removed by magnetic racks and supernatants recovered. Two consecutive immunoprecipitations were performed to completely remove endogenous cyclin A, Bora, Plx1, Tpx2, Plkk, cdk2, cyclin B1 and cyclin B2 proteins. Bora immunoprecipitation was performed using antibodies raised against GST-full length Xenopus Bora whereas western blot was performed with antibodies against Xenopus-Nter-Bora.

Casein and H1 Kinase Activities

For Histone 1 kinase assay, cyclin A, cyclin B1 or cyclin B2 immunoprecipitates from 2 activated eggs or 10 μl of interphase extracts were thawed by the addition of 19 μl H1 buffer, including 0.2 μCi of [γ33P]ATP and incubated for 10 minutes at room temperature. Reactions were stopped by adding Laemmli sample buffer and analysed by SDS-PAGE. For Plx1 activity, Plx1 immunoprecipitates from 10 μl of extracts or from 2 activated oocytes were mixed with a buffer containing 1mg/ml of dephosphorylated α-casein, 0,2 μl of 3.33 μM [γ33P]ATP (200 cpm/picomole), 2 mM $MgCl_2$, 50 mM Tris-HCL pH7,5 and incubated for 20 minutes at room temperature. Incubation were stopped by the addition of Laemmli buffer and analysed by SDS-PAGE and autoradiography.

In Vitro Phosphorylation

Cyclin A immunoprecipitates from 20 μl of interphase extracts were used to phosphorylate 250 ng of recombinant Plx1 or Bora (1-224) in a final volume of 10 μl of phosphorylation mix (20 mM HEPES, 10 mM $MgCl_2$, 100 μM ATP) and 2 μCi of [γ-33P]ATP. Twenty minutes later, reactions were stopped by adding Laemmli sample buffer and analyzed by SDS-PAGE.

Thio-Phosphorylation of Xenopus Bora (1-224)

20 μl of magnetic protein G-Dynabeads (Dynal) prebound to 3 μg of anti-Xenopus cyclin A antibodies were mixed with 20 μl of interphase extracts and incubated for 30 minutes. The immunoprocepitate was then washed with 50 mM Tris pH 7.5, 300 mM NaCl, and mixed with 5 μg of Bora (1-224) in 40 μl of phosphorylation buffer (10 mM Tris pH 7.5, 20 mM βGlycerophosphate, 30 mM NaCl, 10 mM KCl, 5 mM $MgCl_2$, 0.5 mM EGTA, 0.5 mM $ATP^{\gamma S}$, ,1 mM DTT and 30 mM Okadaic Acid). After overnight incubation at room temperature the mix was dialysed twice for 1 hour in a volume of 1 l of 20 mM TrisHCl, 150 mM NaCl and 0.01% tween 20 at room temperature.

Plasmids, Antibodies and Immunoblots

1 μl of interphase or CSF egg extracts was loaded on a polyacrylamide gel and transferred onto Immobilon-P. Membranes were blocked with 5% milk-TBST, incubated with primary antibodies in 2% milk-TBST. HRP conjugated secondary antibodies directed against rabbit (Cell Signaling) and mouse (Santa Cruz biotechnologies) or RecA-HRP (Invitrogen) were incubated 40 min at RT in 2% milk-TBST.

Xenopus Plkk was amplified from PCR4 Topo Plkk plasmid (Biovalley) using indicated primers and subcloned into pGEX4T1 using BamHI-XhoI cloning site. Plasmids used are indicated in supplementary Table S2.

Xenopus full length Bora cDNA was amplified from Xenopus ovary cDNAs and subcloned blunt into EcoRV cloning site pCS2 and subsequently amplified from this plasmid by PCR using specific antibodies (Key Resource Table) and subcloned either in EcoRI-HindIII cloning site of pMalP2 or in EcoRI-NotI cloning site of pGEX4T1. Bora (1-224) sequence was amplified from pCS2-Xenopus Bora and subcloned in the pMalC2x plasmid in the BamHI-SalI site.

Antibody Production and Purification

MBP or GST fusion proteins were expressed in *E. coli* and purified by amylose or glutathione columns respectively. Purified proteins were then supplemented to the extracts or used for rabbit immunization respectively. Serum was finally affinity purified on immobilised recombinant fusion proteins.

For anti-peptide directed antibodies, peptides were coupled to thyroglobulin using sulfo-MBS for immunisation and CNBr-sepharose-immobilised BSA for affinity purification as previously described (Lorca et al., 1998).

Site-Directed Mutagenesis

Deletions and point or triple mutations of Xenopus Bora were obtained by using the Pfu ultra II fusion DNA polymerase (Agilent). Oligonucleotides used for site directed mutagenesis were purchased from Eurogentec and are detailed in the Key Resource Table.

Purification of Human Cyclin A

BL21 bacteria expressing human cyclin A were sonicated and centrifuged 100 000 g for 1 h. Supernatant was recovered and precipitated with 30% ammonium sulphate. Supernatant was then recovered, dialysed for 3 h in a buffer containing 50 mM Tris pH 7.5 and subsequently centrifuged again for 15 min at 100 000 g. Supernatant was then loaded in a MonoQ-4,6/100 (GE Healthcare Life Science) and eluted in a gradient of NaCl from 0 to 1M NaCl. 10 μl from a total of 800 μl of the eluted fractions were used for PAGE-Electrophoresis and Coomassie blue staining to check cyclin A purification.

Mathematical Modelling

The mathematical model is a set of ordinary differential equations. The simulation, parameter estimation, and bifurcation analysis of the model were performed using MATLAB and Optimization Toolbox Release 2013b, The MathWorks, Inc., Natick, Massachusetts, United States.

Model Construction

We have built a simplified mathematical model describing the main regulatory events that trigger the mitotic entry. Contrary to more comprehensive cell cycle models that contain tens of variables and ordinary differential equations (ODEs), this model contain only a few variables and ODEs. This choice is justified by the fact that simplified models including essential regulations behave very similarly to more complex models. Furthermore, for our data, we were limited in the number of variables that we can monitor experimentally. Therefore, it would have been impossible, using our data, to discriminate between simple and more complex models. This simple model has been used to show that our data is compatible with the proposed mechanism for mitotic entry. The model also allowed us to get a better theoretical understanding of the cell cycle dynamics before and during the mitotic entry.

The model is composed of two parts. The first part describes the activation and inactivation of the cyclin B/Cdk1 (MPF) complexes triggered by p-Plx1. We consider that the transition from inactive to active cyclin B/Cdk1 is induced by the active form of Cdc25. The reverse transition is induced by the active form of Wee1. We considered that the cyclin B and therefore MPF is produced at constant rate during G2 phase and mitotic entry. This standard picture can be simply described by two ordinary differential equations:

$$\frac{dMPF_a}{dt} = k_1[Cdc25_a]MPF_i - k_2[Wee1_a]MPF_a - Proteolysis_a, \qquad \text{(Equation S1.1)}$$

$$\frac{dMPF_i}{dt} = Production + k_2[Wee1_a]MPF_a - k_1[Cdc25_a]MPF_i - Proteolysis_i, \quad \text{(Equation S1.2)}$$

where k_i, $1 \leq i \leq 2$ are parameters; the *Production* term corresponds to synthesis of cyclin B during the G2 phase and the *Proteolysis* term corresponds to the cyclin degradation at the mitotic exit.

Similarly to existing models (Tsai et al., 2014) we chose not to use ODEs for describing the dynamics of $[Cdc25_a]$ and $[Wee1_a]$. These variables are considered to be tied to MPF_a that rapidly regulates their level. The concentration of $Cdc25_a$ is an increasing function of MPF_a. Furthermore, we considered that $Cdc25_a$ is also an increasing function of *p-Plx1*. The latter feature represents one of the novelties introduced by our modeling with respect to previous models in the literature. The concentration of active Wee1 is a decreasing function of MPF_a. The experimental data suggests that the response of Cdc25 and Wee1 to its regulators is thresholded. We therefore used Hill functions to describe the activation of these components. Furthermore, we considered that Cdc25 has a MPF_a independent basal activity in the presence of p-Plx1 and no activity at all in the absence of p-Plx1. Thus, we propose the following model:

$$[Cdc25_a](MPF_a, [p-Plx1]) = \left(B + \frac{MPF_a^{n_1}}{\theta_1^{n_1} + MPF_a^{n_1}}\right) \times \frac{[p-Plx1]^{n_2}}{\theta_2^{n_2} + [p-Plx1]^{n_2}}, \quad \text{(Equation S1.3)}$$

$$[Wee_a](MPF_a) = \frac{\theta_3^{n_3}}{\theta_3^{n_3} + MPF_a^{n_3}}, \quad \text{(Equation S1.4)}$$

where n_i, $1 \leq i \leq 3$ are Hill indices and θ_i, $1 \leq i \leq 3$ are thresholds defined as concentrations of regulators at half maximum of activity and B is the maximal activity of Cdc25 in the absence of MPF_a. The Hill indices control the steepness of the regulation (if they are high the activity changes steeply with the concentration of the regulators), whereas the thresholds locate the change of activity in the concentration space.

In order to cover the G2 phase and mitosis we also model the *Production* and *Proteolysis* terms. We will consider the cyclin B production to be constant during G2, thus

$$Production = k_0. \quad \text{(Equation S1.5)}$$

Proteolysis of cyclin B is induced by the anaphase-promoting complex APC/C that is controlled by the polo-like kinase (Castro et al., 2005). A simple model for this term is the following:

$$Proteolysis_a = k_3 MPF_a \frac{[p-Plx1]^{n_4}}{\theta_4^{n_4} + [p-Plx1]^{n_4}},$$

$$Proteolysis_i = k_3 MPF_i \frac{[p-Plx1]^{n_4}}{\theta_4^{n_4} + [p-Plx1]^{n_4}}. \quad \text{(Equation S1.6)}$$

With these remarks, the two Equations S1.1 and S1.2 become

$$\frac{dMPF_a}{dt} = k_1\left(B + \frac{MPF_a^{n_1}}{\theta_1^{n_1} + MPF_a^{n_1}}\right) \times \frac{[p-Plx1]^{n_2}}{\theta_2^{n_2} + [p-Plx1]^{n_2}} MPF_i - k_2 \frac{\theta_3^{n_3}}{\theta_3^{n_3} + MPF_a^{n_3}} MPF_a - k_3 MPF_a \frac{[p-Plx1]^{n_4}}{\theta_4^{n_4} + [p-Plx1]^{n_4}} \quad \text{(Equation S1.7)}$$

$$\frac{dMPF_i}{dt} = k_0 + k_2 \frac{\theta_3^{n_3}}{\theta_3^{n_3} + MPF_a^{n_3}} MPF_a - k_1\left(B + \frac{MPF_a^{n_1}}{\theta_1^{n_1} + MPF_a^{n_1}}\right) \times \frac{[p-Plx1]^{n_2}}{\theta_2^{n_2} + [p-Plx1]^{n_2}} MPF_i - k_3 MPF_i \frac{[p-Plx1]^{n_4}}{\theta_4^{n_4} + [p-Plx1]^{n_4}} \quad \text{(Equation S1.8)}$$

The second part of our model describes the Bora-dependent activation of Plx1 by the active cyclin A/cdk1 complex.

Plx1 is phosphorylated by Aurora in the presence of Bora and dephosphorylated by PP2A (Wang et al., 2015). We consider that Aurora is constant. Our data shows that the p-Plx1 signal is always delayed with respect to the p-Bora signal. Furthermore, there is no p-Plx1 signal if p-Bora is low, suggesting the existence of a p-Bora threshold for Plx1 phosphorylation. This justifies the use of a Hill function in the production term. The resulting equation reads

$$\frac{d[p-Plx1]}{dt} = k_4[Aurora]\frac{[p-Bora]^{n_5}}{\theta_7^{n_5} + [p-Bora]^{n_5}} - k_5[PP2A][p-Plx1]. \quad \text{(Equation S1.9)}$$

PP2A has a behavior similar to $Wee1_a$ being rapidly inhibited by MPF_a, therefore:

$$[PP2A] = \frac{\theta_6^{n_6}}{\theta_6^{n_6} + MPF_a^{n_6}} \quad \text{(Equation S1.10)}$$

The levels of p-Bora are controlled by phosphorylation by active cyclin A/cdk1. We suppose that the phospho- rylation of Bora is fast which allows us to write that p-Bora is proportional to active cyclin A/cdk1. It follows that

$$[p-Bora]=k_6[cycA-cdk1_a]. \quad \text{(Equation S1.11)}$$

Then Equation S1.9 becomes

$$\frac{d[p-Plx1]}{dt}=k_4[Aurora]\frac{[cycA-cdk1_a]^{n_5}}{\theta_5^{n_5}+[cycA-cdk1_a]^{n_5}}-k_5\frac{\theta_6^{n_6}}{\theta_6^{n_6}+MPF_a^{n_6}}[p-Plx1] \quad \text{(Equation S1.12)}$$

where $\theta_5 = \theta_7/k_6$.

The resulting model has 3 differential equations, namely Equations S1.7, S1.8, and S1.12.

Data Normalization

Data was normalized between 0 and 1 by dividing the value of each variable by its maximum all data confounded. The variable *pTyr* (representing MPF_i) was further rescaled to cope with the constraint $MPF_i \leq MPF_{tot}$ where MPF_{tot} is represented by *CycB*. The normalized data is represented in Figure S1.

Parameter Estimation

The parameter procedure estimation is entirely automatic and has been performed using MATLAB and Optimization Toolbox Release 2013b, The MathWorks, Inc., Natick, Massachusetts, United States.

The full model has 19 parameters. These were estimated in two steps. In the first step we estimated 13 parameters of the partial model made by the first two Equations S1.7 and S1.8 with *[p-Plx1](t)* considered as input. The estimation method was the minimisation of an objective function $O(p)$ defined as the l^2 (sum of squares) distance between experimental data and model prediction. The input profile $[p\text{-}Plx1](t)$ was interpolated from data using the MATLAB function interp1 with a piecewise cubic method. The optimisation was performed using the MATLAB function lsqnonlin starting from 100, different, randomly chosen initial parameter values. The best optimum p_{opt} was kept as parameter estimate. We also kept local optima where the objective function is at most 50% higher than the global optimum. These local optima were used to define the confidence interval as $[p_{min},p_{max}]$, where $p_{min}=min\{p|\ O(p) < 1.5O(p_{opt})\}$, $p_{max} = max\{p\ |\ O(p) < 1.5O(p_{opt})\}$. The optimization used data sets coming from a single experiment or combined data sets produced in two experiments when this was possible. The result of the parameter estimates for various data sets is given in the Table S1. The goodness of fit is illustrated in Figure S2.

The remaining 6 parameters occurring in (Equation S1.12) where estimated in a second step by comparing experimental data with the solution of the full system of 3 Equations S1.7, S1.8, and S1.12 with the input $[cycA\text{-}cdk1_a]$. After data normalisation (see previous section) the maximum values are the same (equal to one) for $[cycA\text{-}cdk1_a]$ and [*p-Bora*], therefore k_6=1 and [*p-Bora*] can replace $[cycA\text{-}cdk1_a]$ as input. During the second optimisation step the 13 already estimated parameters were considered known and fixed. This second step was possible only for experimental data sets that include $[cycA\text{-}cdk1_a]$ or [*p-Bora*] time series together with $[p\text{-}Plx1](t)$, MPF_a and MPF_i time series. The result of the parameter estimates is given in the Table S2. The goodness of fit is illustrated in Figure S3.

Bifurcations and Hysteresis at Mitotic Entry

The purpose of this section is to compute hysteresis curves analytically. Computing hysteresis curves boils down to computing steady states. In slow/fast systems this is slightly more complicated: instead of steady states one has to compute constrained steady states. The reason, explained in simple words, is that fast/slow systems have two types of variables. The fast variables equilibrate very rapidly and satisfy steady state equations. The slow variables do not have time to equilibrate, therefore their values have to be set to constants. Equating slow variables to constants are extra constraints, hence the method can be called constrained steady state calculation.

We compute constrained steady states of the full model and of the partial model. The slow variable in our model is the total cyclin B (MPF_{tot}). Thus, the constraint is as follows:

$$MPF_i+MPF_a=MPF_{tot}=const., \quad \text{(Equation S1.13)}$$

allowing to eliminate one variable by expressing it as $MPF_i = MPF_{tot} - MPF_a$.

Equation S1.7 becomes

$$\frac{dMPF_a}{dt}=k_1\left(B+\frac{MPF_a^{n_1}}{\theta_1^{n_1}+MPF_a^{n_1}}\right)\times\frac{[p-Plx1]^{n_2}}{\theta_2^{n_2}+[p-Plx1]^{n_2}}(MPF_{tot}-MPF_a)-k_2\frac{\theta_3^{n_3}}{\theta_3^{n_3}+MPF_a^{n_3}}MPF_a-k_3MPF_a\frac{[p-Plx1]^{n_4}}{\theta_4^{n_4}+[p-Plx1]^{n_4}}. \quad \text{(Equation S1.14)}$$

Setting $\frac{dMPF_a}{dt}=0$ in (Equation S1.14) we obtain the equation of the hysteresis curve relating MPF_a and MPF_{tot} at fixed $[p-Plx1]$:

$$MPF_{tot}=MPF_a\left[1+\frac{\left(\theta_2^{n_2}+[p-Plx1]^{n_2}\right)\left(k_2\frac{\theta_3^{n_3}}{\theta_3^{n_3}+MPF_a^{n_3}}+k_3\frac{[p-Plx1]^{n_4}}{\theta_4^{n_4}+[p-Plx1]^{n_4}}\right)}{k_1[p-Plx1]^{n_2}\left(B+\frac{MPF_a^{n_1}}{\theta_1^{n_1}+MPF_a^{n_1}}\right)}\right]. \quad \text{(Equation S1.15)}$$

Setting $\frac{d[p-Plx1]}{dt}=0$ in (Equation S1.12) we obtain:

$$[p-Plx1]=\frac{[k_4 Aurora]}{k_5}\frac{[cycA-cdk1_a]^{n_5}}{\theta_5^{n_5}+[cycA-cdk1_a]^{n_5}}\frac{\theta_6^{n_6}+MPF_a^{n_6}}{\theta_6^{n_6}} \quad \text{(Equation S1.16)}$$

Combining Equations S1.15 and S1.16 we obtain the equation of the hysteresis curve relating MPF_a and MPF_{tot} at fixed [*cycA*-*cdk*1$_a$].

QUANTIFICATION AND STATISTICAL ANALYSIS

In Figure 2B, autoradiography bands were measured and represented as mean +/- standard deviation derived from three biological replicates.

DATA AND SOFTWARE AVAILABILITY

All analyses were performed using Excel and PowerPoint 14.7.7 (Microsoft), ImageJ 1.5i (NIH), Adobe Photoshop CS5 12.0x64, MATLAB and Optimization toolbox Release 2013b (The MathWorks, Inc, Natick, Massachusetts, US).